EPA-600/2-77-209a
October 1977

Environmental Protection Technology Series

GAS-ATOMIZED SPRAY SCRUBBER EVALUATION

Industrial Environmental Research Laboratory
Office of Research and Development
U.S. Environmental Protection Agency
Research Triangle Park, North Carolina 27711

RESEARCH REPORTING SERIES

Research reports of the Office of Research and Development, U.S. Environmental Protection Agency, have been grouped into nine series. These nine broad categories were established to facilitate further development and application of environmental technology. Elimination of traditional grouping was consciously planned to foster technology transfer and a maximum interface in related fields. The nine series are:

1. Environmental Health Effects Research
2. Environmental Protection Technology
3. Ecological Research
4. Environmental Monitoring
5. Socioeconomic Environmental Studies
6. Scientific and Technical Assessment Reports (STAR)
7. Interagency Energy-Environment Research and Development
8. "Special" Reports
9. Miscellaneous Reports

This report has been assigned to the ENVIRONMENTAL PROTECTION TECHNOLOGY series. This series describes research performed to develop and demonstrate instrumentation, equipment, and methodology to repair or prevent environmental degradation from point and non-point sources of pollution. This work provides the new or improved technology required for the control and treatment of pollution sources to meet environmental quality standards.

REVIEW NOTICE

This report has been reviewed by the participating Federal Agencies, and approved for publication. Approval does not signify that the contents necessarily reflect the views and policies of the Government, nor does mention of trade names or commercial products constitute endorsement or recommendation for use.

This document is available to the public through the National Technical Information Service, Springfield, Virginia 22161.

EPA-600/2-77-209a
October 1977

GAS-ATOMIZED SPRAY SCRUBBER EVALUATION

by

Seymour Calvert, Harry F. Barbarika, and Gary M. Monahan

Air Pollution Technology, Inc.
4901 Morena Boulevard (Suite 402)
San Diego, California 92117

Contract No. 68-02-1869
ROAP No. 21ADM-029
Program Element No. 1AB012

EPA Project Officer: Dale L. Harmon

Industrial Environmental Research Laboratory
Office of Energy, Minerals, and Industry
Research Triangle Park, N.C. 27711

Prepared for

U.S. ENVIRONMENTAL PROTECTION AGENCY
Office of Research and Development
Washington, D.C. 20460

ABSTRACT

Fine particle collection efficiency measurements were made on a gas atomized spray scrubber which cleaned the effluent gas from a No. 7 gray iron cupola. Tests were made at several levels of pressure drop and liquid/gas ratio. Particle size measurements on inlet and outlet gas streams were made with cascade impactors and an A.P.T. screen type diffusion battery.

The particle mass collection efficiency at a pressure drop of about 100 cm W.C. was 91% for particles with a mass median diameter of about 0.4 μmA. Scrubber inlet gas flow rate could vary because the cupola was operated with an open top and it ranged from 4.0 to 12.6 Am^3/s (8,500 to 27,000 ACFM). Air leakage into the scrubber system caused serious operating problems until most of the leaks were sealed.

The penetrations for 1 μmA diameter particles were about as predicted by the mathematical model, while smaller particle penetrations were lower and larger particle penetrations higher than predicted. The latter two effects are believed due to water condensation effects and entrainment, respectively.

This report was submitted in partial fulfillment of Contract No. 68-02-1869 by Air Pollution Technology, Inc. under sponsorship of the U.S. Environmental Protection Agency.

TABLE OF CONTENTS

LIST OF FIGURES

FIGURES (CONTINUED)

LIST OF TABLES

TABLES (CONTINUED)

SECTION 1

INTRODUCTION

Air Pollution Technology, Inc. (A.P.T.) conducted a performance evaluation of a gas-atomized spray scrubber in accordance with EPA Contract Number 68-02-1869 "Fine Particle Scrubber Evaluation". The scrubber controlled emissions from a No. 7 gray iron cupola.

The objective of this performance test was to determine fine particle collection efficiency as a function of particle size and scrubber operating parameters.

Simultaneous inlet and outlet particle sampling measurements were taken on the scrubber during a two-week test period from February 21 to March 4, 1977. Cascade impactor, condensation nuclei counters, and a portable diffusion battery were used to obtain total mass loadings and size distribution data. The data and results of this scrubber evaluation are presented in this text.

SECTION 2

SUMMARY AND CONCLUSIONS

Fine particle collection efficiency measurements were made on a gas atomized spray scrubber which cleaned the effluent gas from a No. 7 gray iron cupola. Tests were made at several levels of pressure drop and liquid/gas ratio.

The scrubber throat was a rectangular nozzle with a variable outlet width. Hot gas from the cupola passed through an afterburner and then a water spray quencher before reaching the scrubber throat. A cyclone separator located downstream from the scrubber removed liquid from the gas and returned it to the scrubber sump, from which it was pumped back to the scrubber throat.

The penetrations for 1 μmA diameter particles were about as predicted by the mathematical model, while smaller particle penetrations were lower and larger particle penetrations higher than predicted. The latter two effects are believed due to water condensation effects and entrainment, respectively.

The particle mass collection efficiency at a pressure drop of about 100 cm W.C. was 91% for particles with a mass median diameter of about 0.4 μmA. Scrubber inlet gas flow rate could vary because the cupola was operated with an open top and it ranged from 4.0 to 12.6 Am^3/s (8,500 to 27,000 ACFM). Air leakage into the scrubber system caused serious operating problems until most of the leaks were sealed.

Particle size measurements on inlet and outlet gas streams were made with cascade impactors and an A.P.T. screen type diffusion battery. Liquid entrainment was observed in the outlet gas and is evidenced by an appreciable amount of mass collection in the pre-cutter.

The performance tests were done during a period of cold (around 0°C) and windy weather. This caused condensation to occur

through the mechanisms of heat transfer from the gas and liquid through the vessel and ducting walls and gas temperature reduction due to cold air leakage. Consequently the collection efficiency for sub-micron particles was enhanced.

Corrosion of steel vessels and ducting was caused by the absorption of sulfur oxides and collection of salts from the cupola gas in scrubber liquid. Sodium carbonate addition to the scrubber liquid was begun during the test period in order to keep the pH near 7.0 and thereby reduce corrosion. Regularly scheduled cleaning of the scrubber sump was also started in order to reduce solids carry-over with entrainment.

Following the tests, the cupola was outfitted with a water-sealed cap and a closure for the charging door. With these modifications the scrubber is capable of satisfactorily controlling emissions. The entrainment separator efficiency is inadequate and it should be either improved or replaced.

Computation of penetration as a function of particle size was attempted with the use of the Weibull relationship to describe size distribution. The method was not satisfactory for this case and the visual estimation of slopes was used instead.

SECTION 3

SOURCE AND CONTROL SYSTEM

The emission source for this test was a No. 7 gray iron cupola used for an 8 to 9 hour/day operation. The cupola normally is run for 3 days/week, but during the test period it was run for as many days as possible (3 days for the first week, 5 days for the second week). The operation produces 10 to 12 tons per hour of metal from a feed of scrap metal, coke, and limestone.

During the testing period the cupola ran at normal conditions. The particles result from the melting of the scrap and burning of the coke in the cupola. Figure 1 shows a schematic of the entire operation including the scrubber system.

The hot gases from the melting operation enter the afterburner where they are heated to approximately 700-1000°C. The gases are then quenched by city water, which during the test had a flow rate which varied between 0 and 2.6 ℓ/s (4.1 GPM) giving a temperature range of 700°C to 60°C. Scrubber liquor is added just ahead of the throat section (the rate was varied during the testing period from 2.5 ℓ/s to 15.8 ℓ/s). Next the gases enter a variable throat scrubber section which is a rectangular cross-sectioned orifice with a throat height of 91.4 cm (36 inches). The throat width can be varied from 4.2 cm (1.7 in.) to 11.4 cm (4.5 in.). Following the venturi the gases enter a cyclone entrainment separator. An induced draft blower moves the gas through the scrubbing system, powered by a 298 kW (400 HP) motor. From this blower the gases are exhausted through an 11.9 m (39 ft) high, 0.91 m (3 ft) diameter stack.

At the venturi section, scrubber liquor is pumped in through pipes placed directly upstream of the trim tabs. This liquor be-

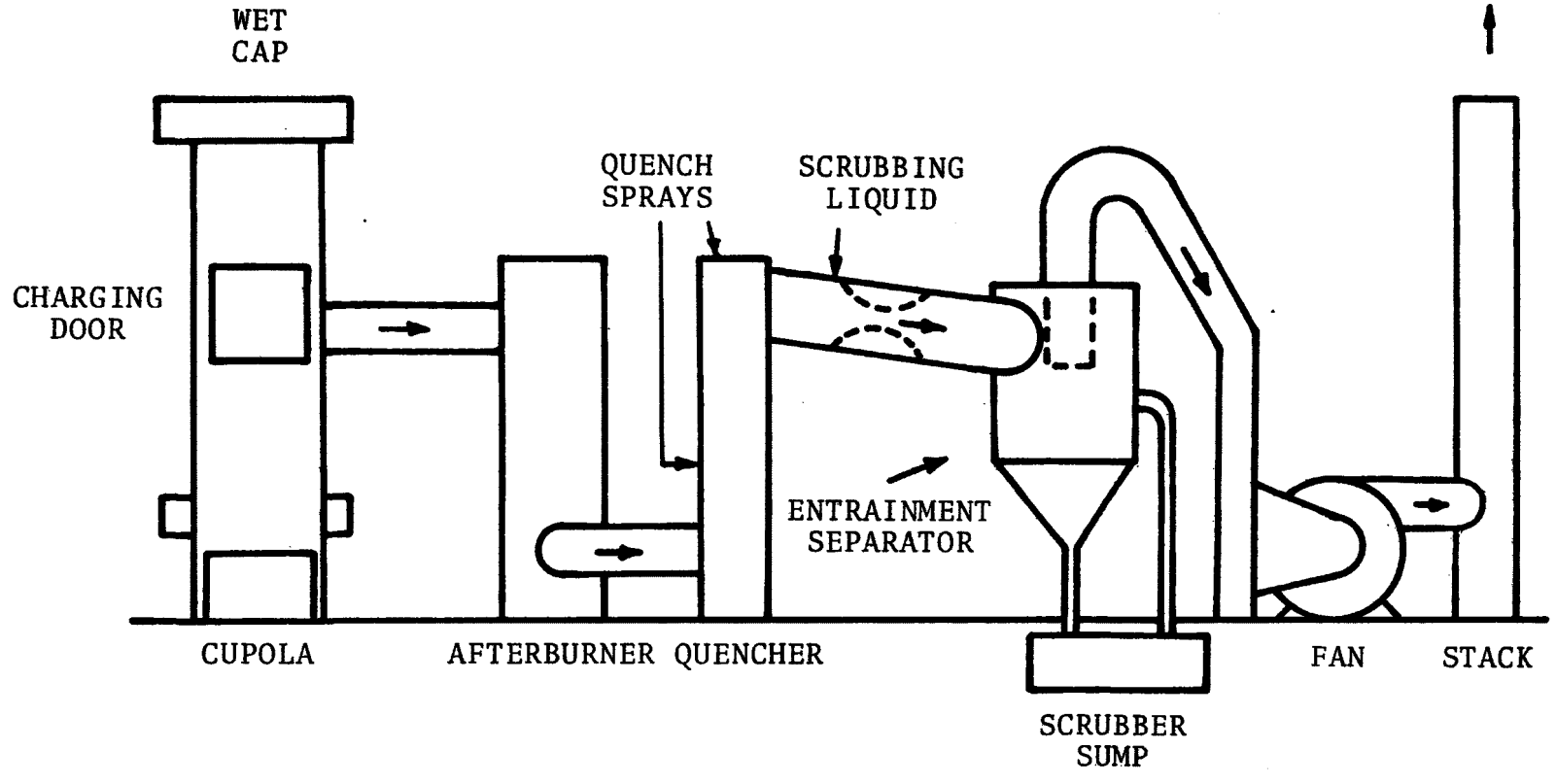

Figure 1. Schematic drawing of scrubber system.

gins as clean water every day from a sump below the cyclone. No fresh water feed is added to this liquor so that as the day progresses the solids concentration increases. When the system is shut down the sump is neutralized, cleaned out, and fresh water pumped in for the next day of operation.

The water used for the quench sprays, however, comes directly from the city water lines and no recirculation is used.

SECTION 4

TEST METHOD

The performance of this gas-atomized spray scrubber was determined from simultaneous measurements of particle size distributions and mass loading of the inlet and outlet gases.

Modified EPA-type sampling trains with heated University of Washington Mark III (U.W.) cascade impactors were used during this test period for particle measurement above 0.2 μmA dia. Figure 2 shows a schematic diagram of the modified sampling train. Outlet impactor runs were performed in-stack, while the inlet runs were ex-stack. The high gas temperatures at the inlet sampling ports prevented in-stack sampling. Glass fiber filter (Gelman type AE) substrates were used in the impactors to prevent particle bounce and minimize wall losses. On the inlet runs low velocity stages were used in the impactor to increase the length of the sampling time.

The Air Pollution Technology portable screen diffusion battery (A.P.T. - S.D.B.) was used for particle measurements from 0.1 μm to 0.01 μm (actual).

The A.P.T. - S.D.B. uses Brownian diffusion to accomplish the size fractionation of particles smaller than 0.1 μm. Because smaller particles diffuse more readily than larger ones, successively larger particles are captured as they proceed through the battery.

A condensation nuclei counter (CNC) was used to determine the particle number concentration at several locations in the battery. From these data the size distribution may be determined for the particles smaller than 0.1 μm. The size distribution computation was based on a calibration of the S.D.B. performed in the A.P.T. laboratory.

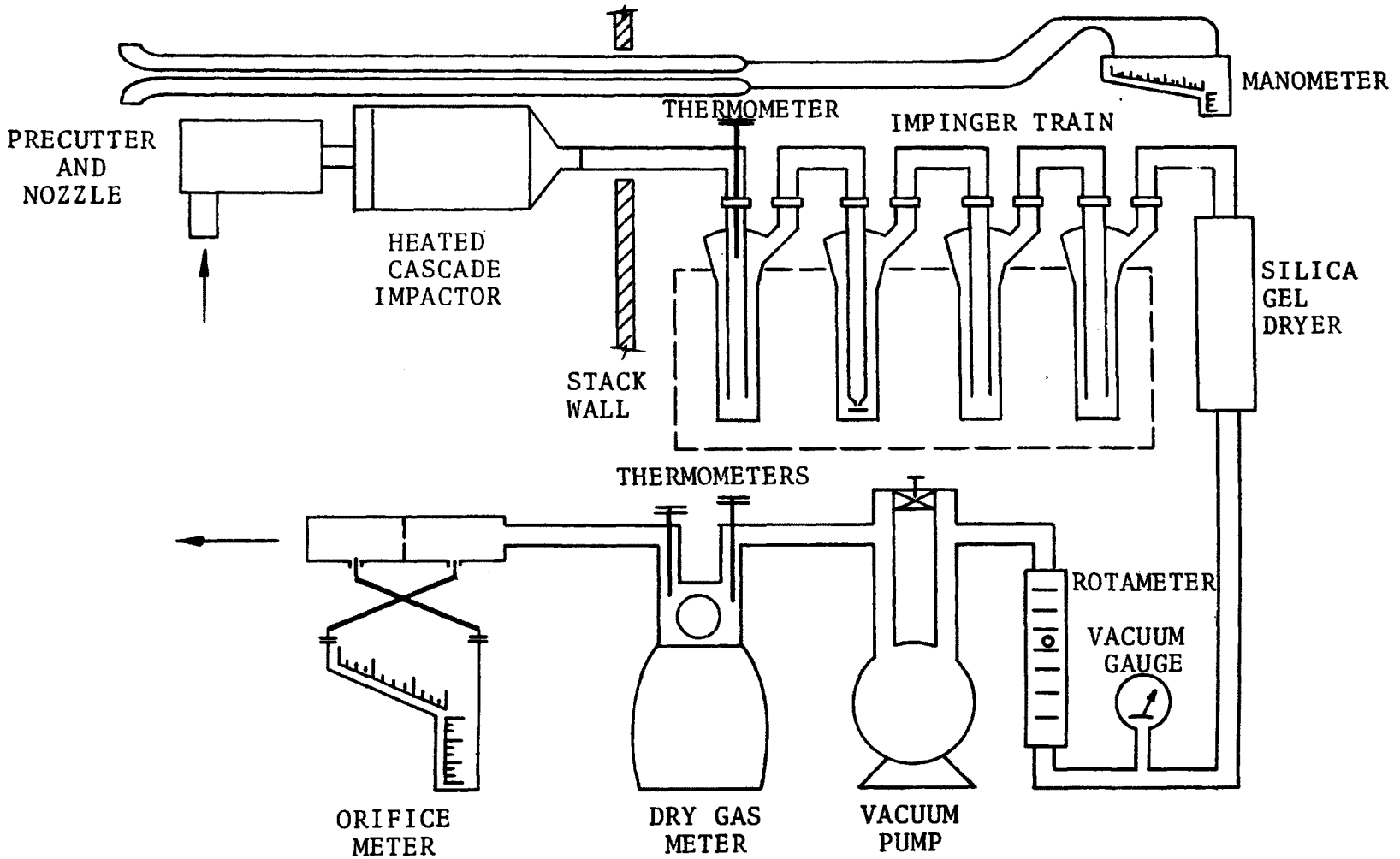

Figure 2 - Modified EPA sampling train with in-stack cascade impactor

During an impactor run, inlet or outlet fine particle size measurements were taken with the portable diffusion battery. Since this cupola has a charging operation to keep the data fairly constant, all impactor runs were started at the beginning of a charge. The diffusion battery data were also taken at the beginning of these charges so that inlet and outlet S.D.B. measurements at different times were considered to approximate simultaneous sampling.

Several impactor blank runs were performed on the inlet and outlet simultaneously to ensure that the stack gases did not react with the substrates. A blank impactor run consisted of a heated impactor preceeded by two heated glass fiber filters run at identical sample conditions as the other regular impactor runs.

Gas flow rates for all tests were determined by means of a calibrated S-type pitot tube. Velocity traverses of the inlet and outlet were performed according to EPA Methods 1 and 2, and average velocity points were selected for single point cascade impactor sampling. Sampling flow rates were maintained with the usual EPA train instruments (rotameter, dry gas meter, and orifice manometer) to obtain isokinetic sampling throughout the entire test. Orsat analyses were performed periodically on both the inlet and outlet gases.

The inlet sample ports, because of a limited length of ducting after quencher and before the venturi throat, were located 0.73 equivalent duct diameters downstream of a 78° bend and 0.73 equivalent duct diameters from the beginning of the venturi section. The inlet duct rectangular (0.91 m x 0.61 m) and its equivalent duct diameter was 0.73 m as calculated by EPA Method 1.

The outlet sample ports were located in a 0.91 m (3 ft) diameter round stack, about 8 stack diameters downstream of the inlet from the fan and 3 diameters upstream of the stack exit. The velocity traverses indicated a well-developed flow pattern.

SECTION 5

PROCESS CONDITIONS

During a two-week testing period 17 impactor sampling runs (two of them being blank impactor runs) were made. The scrubber process conditions for the inlet and the outlet are shown in Tables 1 and 2. Runs 1 through 4 represent the scrubber running with a number of leaks, as can be seen by comparing the inlet and outlet flow rates. Between runs 4 and 5 many of the large leaks were patched, resulting in much smoother operation as well as a reduction of the fan amperage, an increase in the inlet flow rate, and reduction in the outlet flow rate.

After patching most of the leaks, more control over the scrubber operation could be maintained. It was then possible to adjust water flow rates as well as the pressure drop across the venturi. This enabled a number of test conditions to be examined. For the most part, the charging operation was fairly constant and did not vary significantly between the runs, except for run 1 when the crane broke and only one charge was added during the entire run. The average barometric pressure during the testing period was 99.36 kPa (29.34 in. Hg)

The inlet humidities from runs 2,9, and 10 were derived from dessicant and impinger weight gains in the sampling train. The inlet humidities for all other runs, except 12 and 14, were calculated as follows:

In runs 9 and 10, when the quencher water was off, the inlet gas temperature was about 700°C (1,300°F), its humidity about 2%. These conditions correspond to a wet bulb (saturation) temperature of 68°C (155°F). The humidities at inlet temperatures above 68°C were then calculated from a psychometric chart, assuming a wet bulb temperature of 68°C. The humidity for runs 12 and 14 were

TABLE 1. SCRUBBER CONDITIONS

Run No.	P_1 *	P_2 *	P_3 *	P_4 *	P_5 *	ΔP *	Throat Width (cm)	Fan Load (kW)	Scrubber Liq.Flow (ℓ/s)	Quench Flow (ℓ/s)
1	-1.8	- 77.5	- 83.8	-137.0	0.9	75.7	11.4	310	3.2	1.1
2	-1.3	- 81.3	- 94.0	-147.0	0.9	80.0	4.4	276	11.4	0.0
3	-3.0	- 57.2	- 63.5	-137.0	1.1	54.2	5.6	285	< 2.5	1.6
4	-2.0	- 64.8	- 78.7	-135.0	1.1	62.8	4.4	294	< 2.5	1.6
5	-6.4	- 83.8	- 96.5	-114.0	-0.1	76.4	11.4	245	12.6	1.6
6	-6.4	- 85.1	- 94.0	-114.0	-0.1	78.7	11.4	242	12.6	1.6
1-B	-6.6	- 87.6	- 96.5	-117.0	-0.1	81.0	11.4	245	12.6	1.6
7	-6.1	- 87.6	- 94.0	-114.0	-0.1	81.5	11.4	242	12.6	1.6
8	-3.8	- 86.4	-107.0	-119.0	-0.1	82.6	5.1	217	9.5	1.6
2-B	-3.6	- 85.1	-109.0	-122.0	-0.1	81.5	5.1	223	9.5	1.6
9	-5.1	- 87.6	-109.0	-124.0	-0.2	82.5	5.6	220	9.5	0.0
10	-4.3	- 85.1	-107.0	-122.0	-0.2	80.8	5.6	223	9.5	0.0
11	-2.3	-105.0	-122.0	-132.0	-0.1	103.0	4.2	211	12.6	2.6
12	-2.5	-105.0	-125.0	-130.0	-0.1	104.0	4.3	217	12.6	2.5
13	-2.8	-107.0	-125.0	-132.0	-0.1	104.0	4.3	217	12.6	2.5
14	-5.8	- 94.0	-109.0	-117.0	-0.1	88.2	11.4	236	15.8	1.7
15	-5.8	- 92.7	-109.0	-117.0	-0.1	86.9	11.4	232	15.8	1.7

P_1 = static pressure before venturi $\Delta P = P_1 - P_2$

P_2 = static pressure after venturi

P_3 = static pressure before fan dampers

P_4 = static pressure after fan dampers

P_5 = static pressure at outlet sampling ports

* = numbers expressed in cm W.C.

TABLE 2. PROCESS CONDITIONS

Run No.	Inlet Temp. °C	Outlet Temp. °C	Inlet Water Vapor Vol.%	Outlet Water Vapor Vol.% **	Inlet Flow Rate Am^3/s (MACFM)	Outlet Flow Rate Am^3/s (MACFM) ***
1	246	56	21	7	5.2(11.0)	11.7(24.8)
2	496	56	11(6*)	7	6.2(13.2)	11.7(24.8)
3	132	57	27	17	6.5(13.7)	12.5(26.5)
4	132	57	27	17	6.5(13.7)	12.5(26.5)
5	177	65	25	20	11.4(24.1)	10.5(22.2)
6	149	65	26	20	11.0(23.4)	10.5(22.2)
1-B	149	65	26	20	11.0(23.4)	10.5(22.2)
7	177	54	25	5	10.8(22.9)	10.0(21.1)
8	177	54	25	5	10.8(22.9)	10.0(21.1)
2-B	177	54	25	5	10.8(22.9)	10.0(21.1)
9	699	58	2*	6	12.6(26.7)	8.1(17.1)
10	677	58	2*	6	12.5(26.4)	8.1(17.1)
11	68	51	27	8	4.1(8.7)	7.0(14.8)
12	60	51	20	8	4.0(8.4)	7.0(14.8)
13	71	51	32	8	4.2(8.8)	7.0(14.8)
14	66	51	25	11	9.1(19.2)	9.8(20.7)
15	177	51	25	11	10.5(22.2)	9.8(20.7)

* Based on sampling train water catch

** Based on wet and dry bulb temperatures

*** MACFM = thousand actual cu.ft/min

those based on the inlet being saturated.

The inlet sampling was done out-of-stack at a lower temperature and condensation could have occurred in the pre-cutter, probe, etc. Run 2 was the only run for which the calculated humidity was greater than that which was based on evaporation of the quench water. At the outlet, wet and dry bulb thermometers were used to measure stack humidity.

The top of the cupola was open, except for a "wet cap". The wet cap consists of baffles and sprays at the top of the cupola and it was operated during the test period. Depending upon the scrubber conditions, varying quantities of visible emission were observed flowing from the wet cap.

The tests were conducted during the winter so that the ambient temperature averaged about 0°C during the testing. This low ambient temperature probably caused the temperature of the gases entering the scrubber to be lower than normal because of heat transfer through duct walls, leakage of cold air, and use of cooler than normal quencher and scrubber water.

The cyclone separator was not operating efficiently during the testing period. It was patched along with the rest of the system after run 4 but it could not be sealed completely as it was in a rather rusted and patchwork condition. Any leakage into the cyclone would disrupt the flow of liquid down the walls and would cause reentrainment. Reentrainment caused by leakage and perhaps poor flow distribution at the inlet, and internal roughness due to scale build-up was clearly noticeable as rain-out from the stack.

The Orsat analyses of the outlet gases are presented in Table 3.

TABLE 3. AVERAGE GAS COMPOSITION

Gas Component	Inlet Volume, % Dry	Outlet Volume, % Dry (Runs 1-4)	Outlet Volume, % Dry (Runs 5-15)
N_2	80.1	80.1	79.6
O_2	6.4	16.9	14.6
CO_2	13.2	3.0	5.8
CO	0.3	0	0
Molecular Wt.	29.9	28.8	29.2

SECTION 6

CASCADE IMPACTOR PARTICLE DATA

Particle size distribution data were obtained for the gas-atomized spray scrubber as described in the Test Method section. Concurrent single point sampling at the average velocity location was performed at the inlet and outlet. However, due to the different mass loading rates the sample duration differed between inlet and outlet. The average sampling times for the inlet and outlet, respectively, were 6.5 and 31 minutes.

Entrained water drops were a problem at both the inlet and outlet, so pre-cutters were used ahead of the impactors during the sampling runs. The aerodynamic cut diameters of these pre-cutters for the inlet and outlet were approximately 11.6 μmA and 5.6 μmA, respectively. Both the inlet and outlet sampling were approximately isokinetic.

Isokinetic conditions are not crucial for sampling fine particles. For example, the error caused by sampling 4 μmA particles at a velocity 50% higher or lower than the gas stream velocity would only be about 2 or 3% of the concentration.

To minimize the possibility of condensation in the outlet impactors and to collect dry particles, the impactors (except run 9 which was below the stack temperature due to a malfunction of the heating blanket) were maintained at about 13.5°C above the gas stream temperature by heating blankets. Because of the temperature fluctuation at the inlet the impactor was kept out of the stack and heated by a heating blanket to an average temperature of 86°C. The pre-cutters in both cases (inlet and outlet) were not heated.

The fact that the impactors were heated should be noted when interpreting the size distribution data. Because of the

presence of a quencher upstream of the scrubber section, the particles may be wet due to condensed or absorbed water when they enter the scrubber. The wet particles would have a different size distribution than those collected in a heated impactor. The wet particle size distribution would have fewer smaller diameters and probably a larger mass median diameter. The runs with the most favorable conditions for wet particles were runs 11-14.

Particle concentration, particle size, and sampled volume for cascade impactor runs are tabulated in the appendix in Tables A-1 through A-15. Size distributions for the impactor runs are given in Figures A-1 through A-15 located in the appendix. Table 4 summarizes the "d_{pg}" and "σ_g" results for the cascade impactor runs using log-probability parameters. The distribution data include only the results of the cascade impactor stage analysis. The pre-cutter and probe weight gains were not used.

WEIBULL DISTRIBUTION

The Weibull distribution is an exponential function with three parameters that make it more versatile than the log-probability function. A description of the Weibull distribution function is given in Appendix "B". Table 5 summarizes the Weibull distribution data and includes the calculated mass median diamter ($d_{p_{50}}$). The linear correlation coefficients are all very good. These parameters were used to plot the Weibull function on the figures in Appendix "A".

AERODYNAMIC PARTICLE DIAMETER

In this report the particle size determined from cascade impactor analysis is presented in units of "μmA". This diameter is the aerodynamic resistance diameter as described in a discussion of aerodynamic diameter convention by Raabe (1976). The relation to geometric diameter is

$$d_{pa} = d_p \, (\rho_p \, C')^{\frac{1}{2}}$$

where d_{pa} = aerodynamic resistance diameter, μmA
d_p = geometric diameter, μm
ρ_p = particle density, g/cm^3
C' = Cunningham slip correction factor

TABLE 4. CASCADE IMPACTOR DATA USING LOG-PROBABILITY ANALYSIS

Run No.	Inlet d_{pg} (μmA)	Inlet σ_g	Outlet d_{pg} (μmA)	Outlet σ_g
1	0.47	2.6	0.86	1.9
2	0.45	2.9	0.76	4.0
3	0.40	2.1	0.38	2.3
4	0.26	2.7	0.58	2.3
5	0.19	3.4	0.36	2.3
6	0.33	2.0	0.43	2.2
7	0.39	2.0	0.41	2.2
8	0.45	2.0	0.39	2.5
9	0.58	2.0	0.49	2.3
10	0.37	2.7	0.35	2.7
11	0.40	2.4	0.53	2.0
12	0.41	2.4	0.43	2.7
13	0.31	2.7	0.41	2.4
14	0.20	4.4	0.43	2.4
15	0.18	4.4	0.49	2.2

TABLE 5. CASCADE IMPACTOR DATA
USING WEIBULL ANALYSIS *

Run No.	Type	$d_{p_{50}}$ (μmA)	d_{po} (μmA)	θ (μmA)	b	LCC **
1	In	0.48	0.06	0.677	0.926	0.99
1	Out	0.72	0.39	1.12	0.457	1.0
2	In	0.45	0.07	0.673	0.806	0.98
2	Out	0.78	0	1.24	0.783	1.0
3	In	0.37	0.13	0.506	0.798	0.98
3	Out	0.36	0.27	0.450	0.510	1.0
4	In	0.26	0.11	0.368	0.682	0.99
4	Out	0.52	0.26	0.711	0.677	1.0
5	In	0.18	0.10	0.266	0.509	0.99
5	Out	0.34	0.29	0.416	0.427	0.99
6	In	0.30	0.14	0.405	0.767	0.98
6	Out	0.38	0.28	0.484	0.487	1.0
7	In	0.33	0.17	0.445	0.657	0.99
7	Out	0.36	0.27	0.460	0.459	1.0
8	In	0.46	0.12	0.612	0.967	0.99
8	Out	0.36	0.33	0.422	0.322	1.0
9	In	0.52	0.28	0.704	0.630	0.99
9	Out	0.43	0.29	0.585	0.501	0.99
10	In	0.32	0.23	0.444	0.451	0.99
10	Out	0.34	0.27	0.432	0.408	1.0
11	In	0.38	0.12	0.542	0.734	0.98
11	Out	0.45	0.33	0.594	0.487	0.99
12	In	0.36	0.16	0.518	0.643	0.98
12	Out	0.40	0.26	0.545	0.519	1.0
13	In	0.29	0.12	0.424	0.648	0.99
13	Out	0.37	0.28	0.488	0.457	1.0
14	In	0.19	0.06	0.325	0.512	0.99
14	Out	0.38	0.28	0.506	0.473	1.0
15	In	0.17	0.09	0.282	0.438	0.98
15	Out	0.42	0.29	0.571	0.471	0.99

* Column headings are defined in Appendix B

** Linear correlation coefficient

SECTION 7

DIFFUSION BATTERY DATA

Diffusion battery data were taken during the second week of testing. Inlet data were taken during runs 5, 6, 1-B, 8, 2-B, 12, and 13. Outlet data were taken between runs 2-B and 9 and during run 11.

A dilution system was used for this testing along with the A.P.T. diffusion battery. A 208 liter (55 gallon) drum was used upstream of the diffusion battery as this dilution system. A sample should not be taken continuously from the stack because the intermittent charging operation can result in rapidly changing readings. A syringe was inserted into the stack several times to withdraw gas samples and these were expelled into the dilution tank. Later this system was switched to a calibrated hand pump. These gas samples were diluted with dry filtered air in the tank and run through the diffusion battery with particle counts being measured with the condensation nuclei counter.

The particle size distributions determined by diffusion battery analysis are given in Table 6. The diffusion battery results are averages of a number of counts during each run and are reduced using a log-normal distribution fit to penetration through successive screens. The geometric count or number mean diameter (d_{pN}) and geometric standard deviation are the log-normal parameters used in Table 6. The cut sizes of the screens ranges between 0.03 μm and 0.23 μm.

TABLE 6. DIFFUSION BATTERY PARTICLE SIZE DISTRIBUTIONS

D.B. Run No.	Impactor Run No.	Type of Run	d_{pN} (μm)	σ_g	Total Particle Count ** No./cm^3
3	5	In	0.070	3.4	9.0×10^6
4	5	In	0.092	12.0	1.1×10^7
5	6	In	0.095	12.0	1.1×10^7
6	1-B	In	0.128	14.0	3.9×10^6
7	8	In	0.072	6.0	2.3×10^6
8	8	In	0.085	2.9	1.3×10^6
9	2-B	In	0.094	11.5	1.1×10^7
10	2-B*	Out	0.057	1.0	5.1×10^6
11	2-B*	Out	0.061	2.5	8.0×10^6
12	2-B*	Out	0.085	4.5	8.3×10^5
13	11	Out	0.090	6.0	7.8×10^5
14	11	Out	0.090	8.9	1.9×10^6
15	12	In	0.086	9.3	2.2×10^7
16	13	In	0.059	6.0	1.5×10^7

* Same condition but not simultaneous.

** Gas conditions: 20°C, 1 atm

SECTION 8

PARTICLE PENETRATIONS

Particle penetrations versus particle aerodynamic diameter were calculated from cascade impactor and diffusion battery cumulative loading data. The penetrations based on diffusion battery data were calculated from log-normal inlet and outlet cumulative distributions. The physical (actual) size distributions from the diffusion battery analysis were converted to aerodynamic by assuming the cupola dust had a particle density of 2.5 g/cm^3.

Calculation of the particle penetration from cascade impactor data was tried using the mathematical relations of the Weibull distribution function. This method was abandoned because in most cases the calculation gave the result that penetration increased as particle size increased. Also, there was often a minimum in the size range between 1 and 2 μmA diameter. The unrealistic penetration curves resulted inspite of the relatively high linear correlation coefficients of the size distributions.

Since the size distributions were also not log-normal, the cascade impactor penetrations presented in Figures 3-9 were calculated graphically. The method involved graphically determining the slope of the cumulative mass loading versus aerodynamic particle diameter curve, drawn from the data presented in Appendix"A". The ratio of the slopes of the outlet curve to the inlet curve at a certain particle size was the penetration for that particle size.

The total mass loadings and overall penetration for the runs are presented in Table 7 . Mass loading and penetration

are also shown without the outlet pre-cutter catch. The reason being that the pre-cutter loading was mostly entrainment carry-over from the cyclone and was not due to scrubber inefficiency.

TABLE 7. MASS LOADING AND OVERALL PENETRATION

Run No.	Mass Loading, mg/DNm³ *			Penetration, %	
	Inlet	Outlet[1]	Outlet[2]	Pt[1]	Pt[2]
1	1,570	212	46.3	13.5	2.9
2	2,120	74.3	36.5	3.5	1.7
3	1,100	280	267	25.5	24.4
4	2,060	176	175	8.5	8.5
5	3,190	609	514	19.1	16.1
6	2,340	341	307	14.6	13.1
1-B	7,030	968	-	13.8	-
7	2,530	234	234	9.3	9.2
8	1,913	320	98.2	16.7	5.1
2-B	1,600	177	-	11.1	-
9	5,070	198	156	3.9	3.1
10	2,620	589	159	22.5	6.1
11	1,750	159	153	9.1	8.7
12	2,370	214	159	9.0	6.7
13	2,500	797	174	31.8	6.9
14	1,450	278	186	19.2	12.8
15	1,240	277	223	22.2	17.9

[1] Including outlet pre-cutter dry weight gain
[2] Without outlet pre-cutter dry weight gain

* N = 0°C, 1 atm

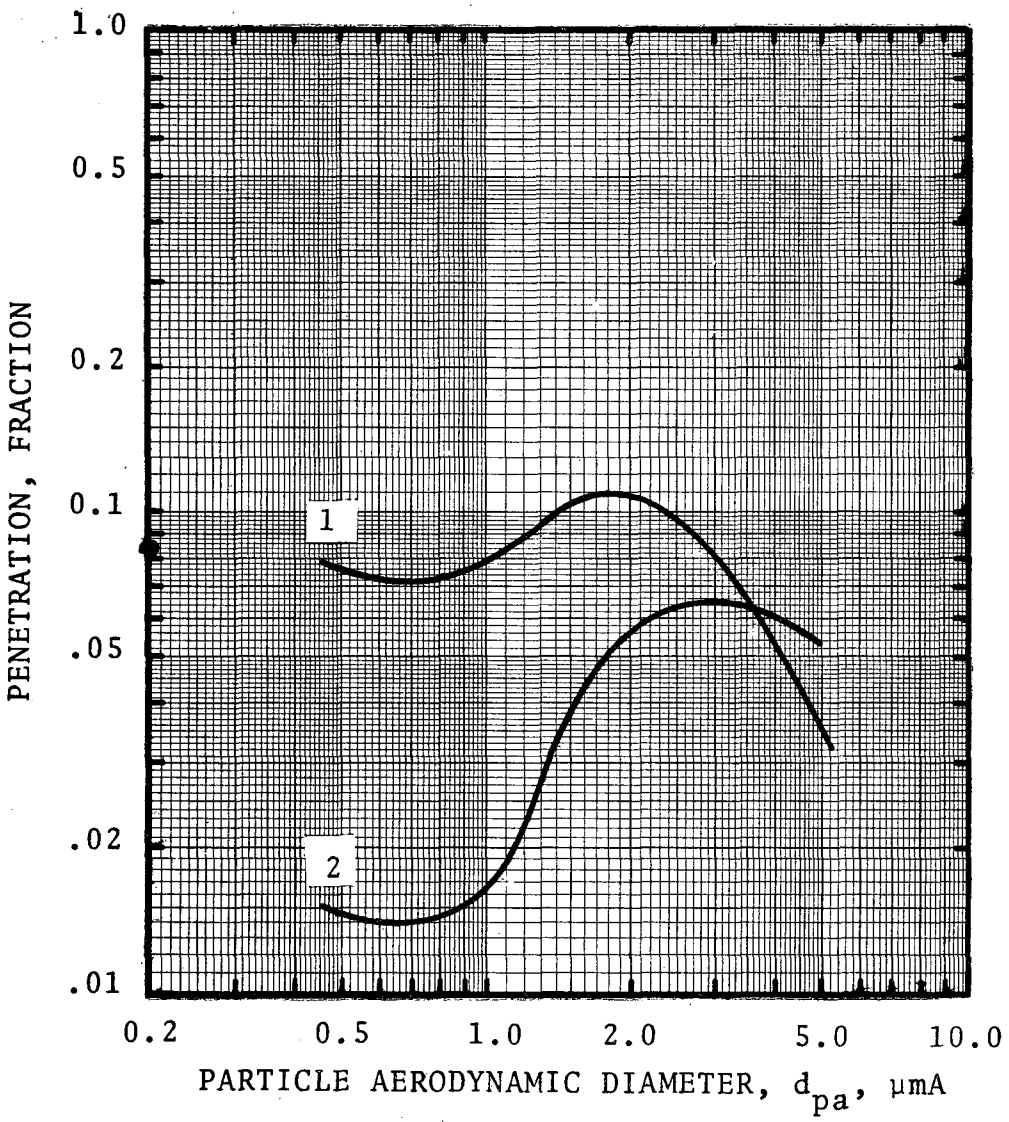

Figure 3. Particle penetration for cascade impactor runs 1 and 2.

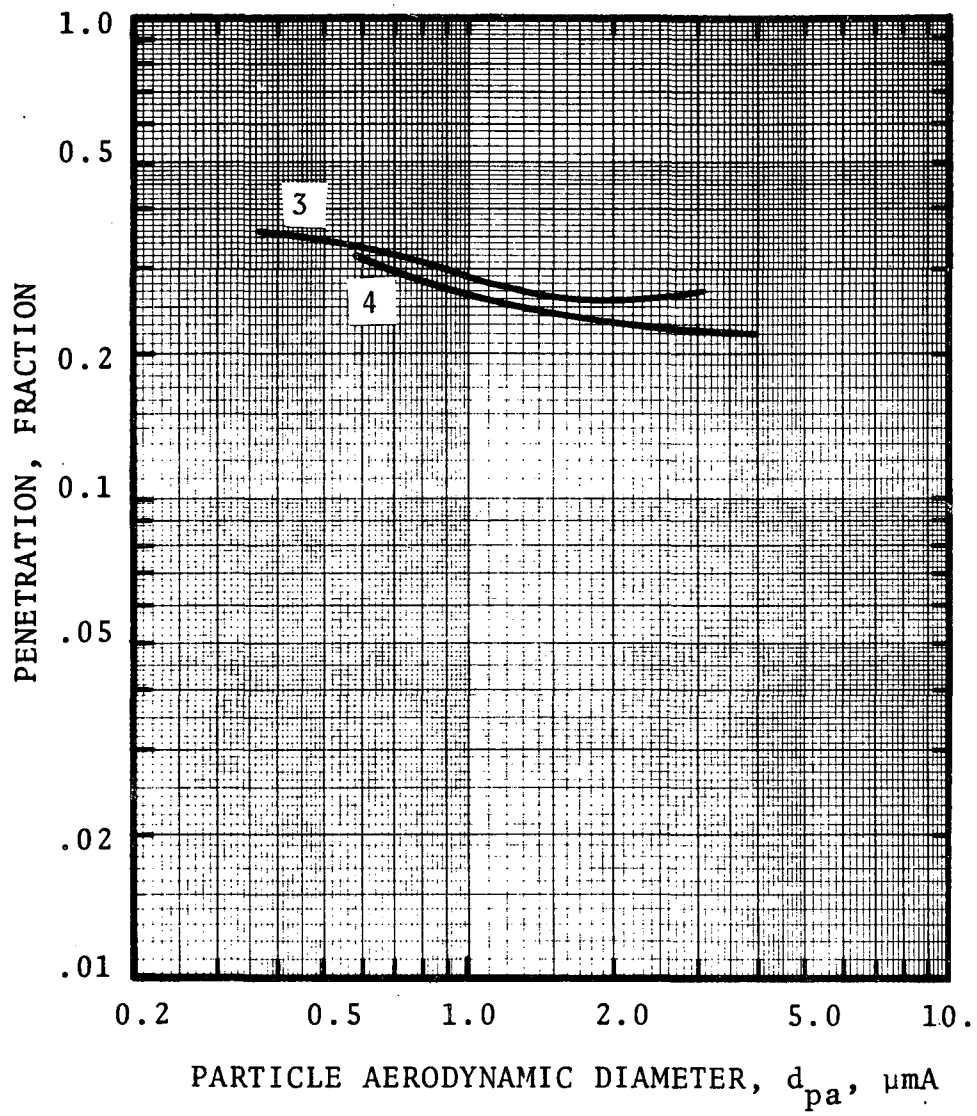

Figure 4. Particle penetration for cascade impactor runs 3 and 4.

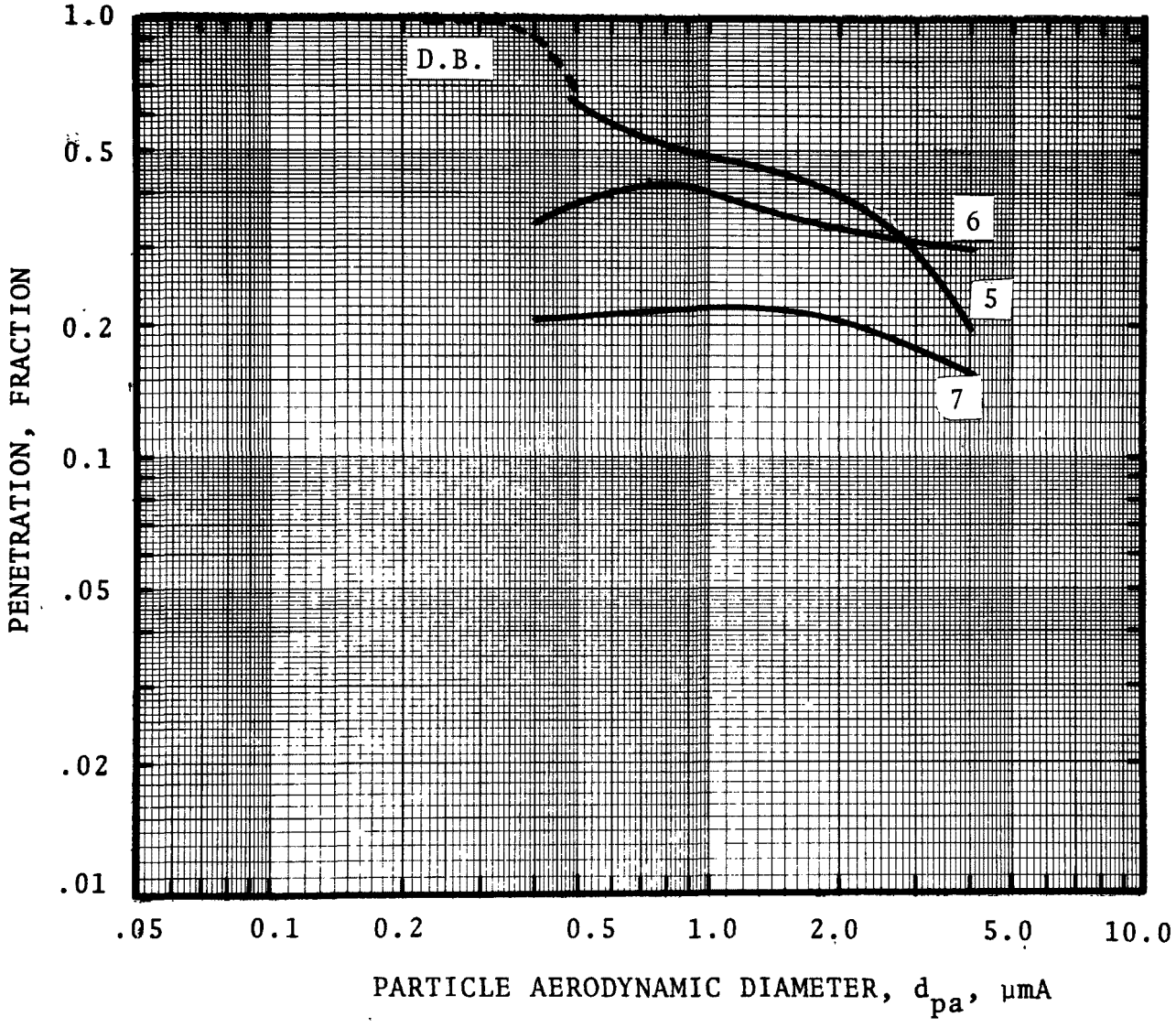

Figure 5. Particle penetration for cascade impactor runs 5, 6 and 7, and diffusion battery runs 3-9 (inlet) and 10-12 (outlet).

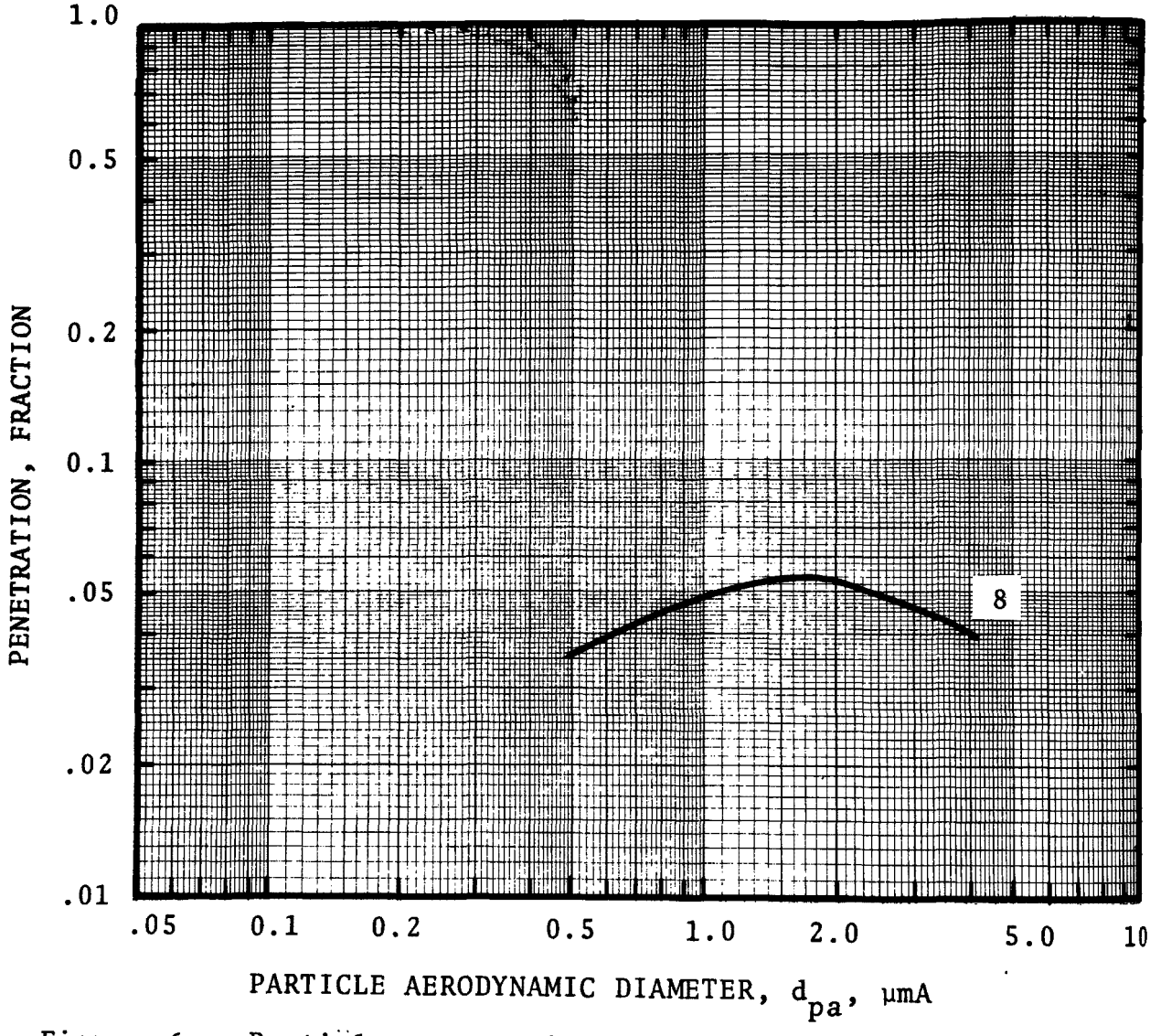

Figure 6. Particle penetration for cascade impactor run 8.

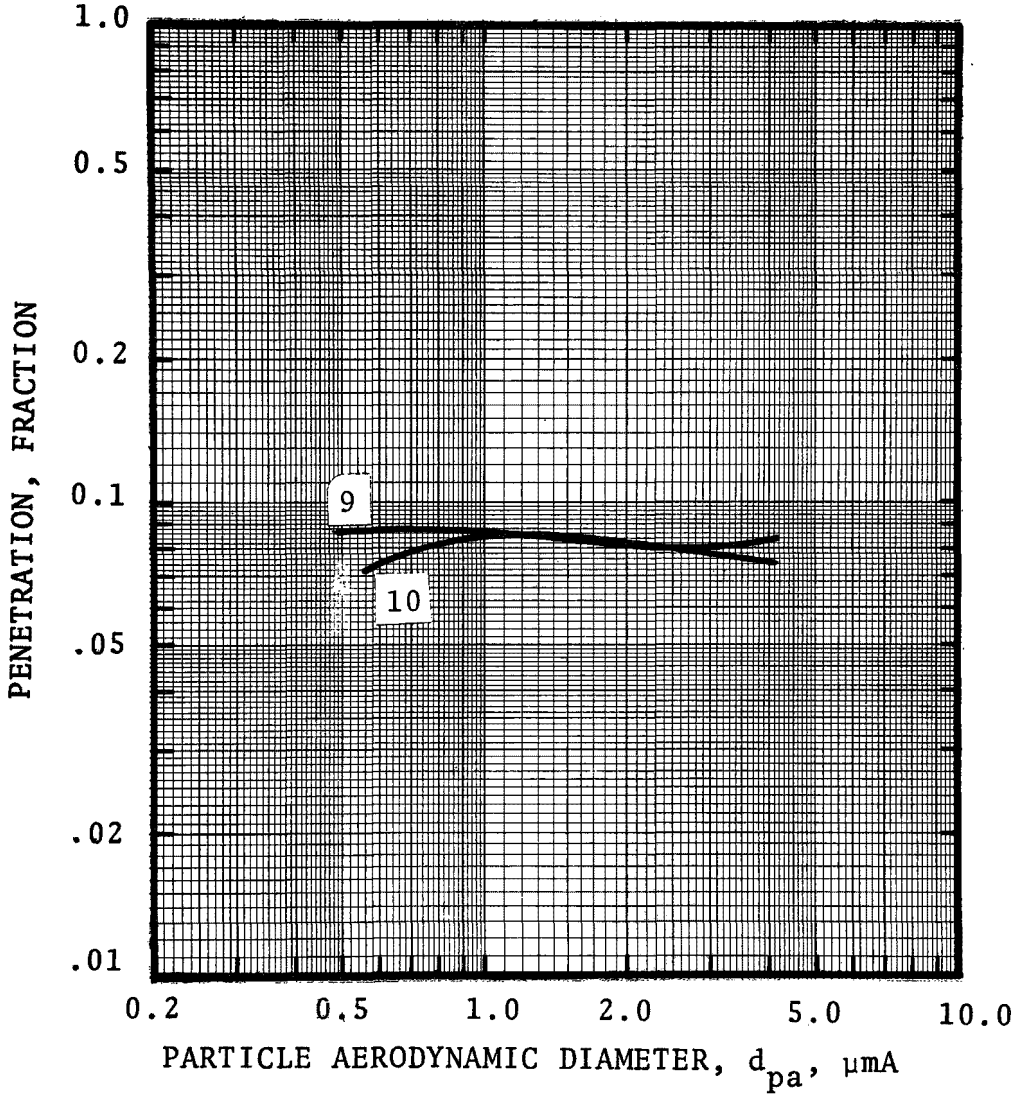

Figure 7. Particle penetration for cascade impactor runs 9 and 10.

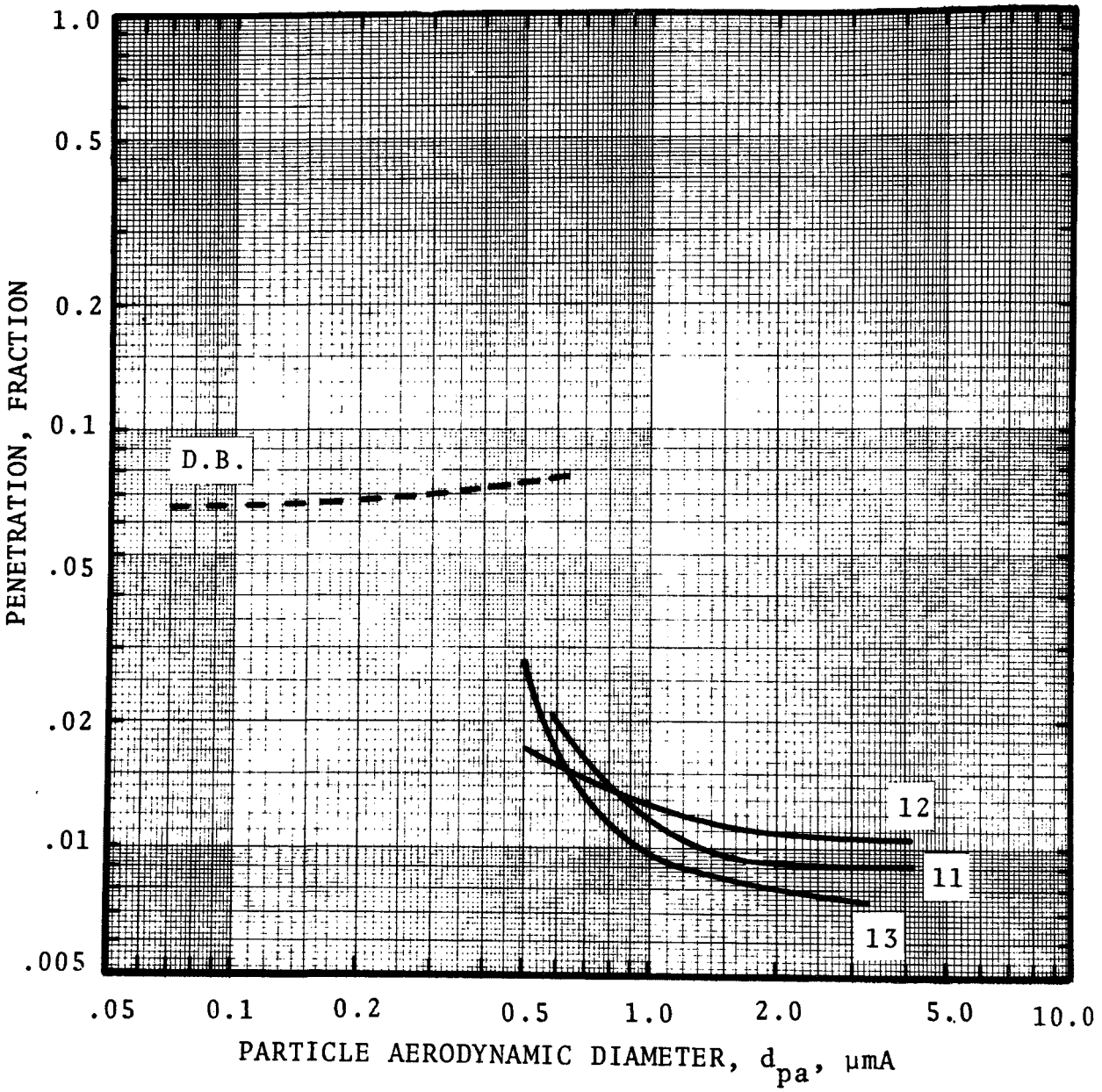

Figure 8. Particle penetration for cascade impactor runs 11, 12 and 13, and diffusion battery runs 15 and 16 (inlet) and 13 and 14 (outlet).

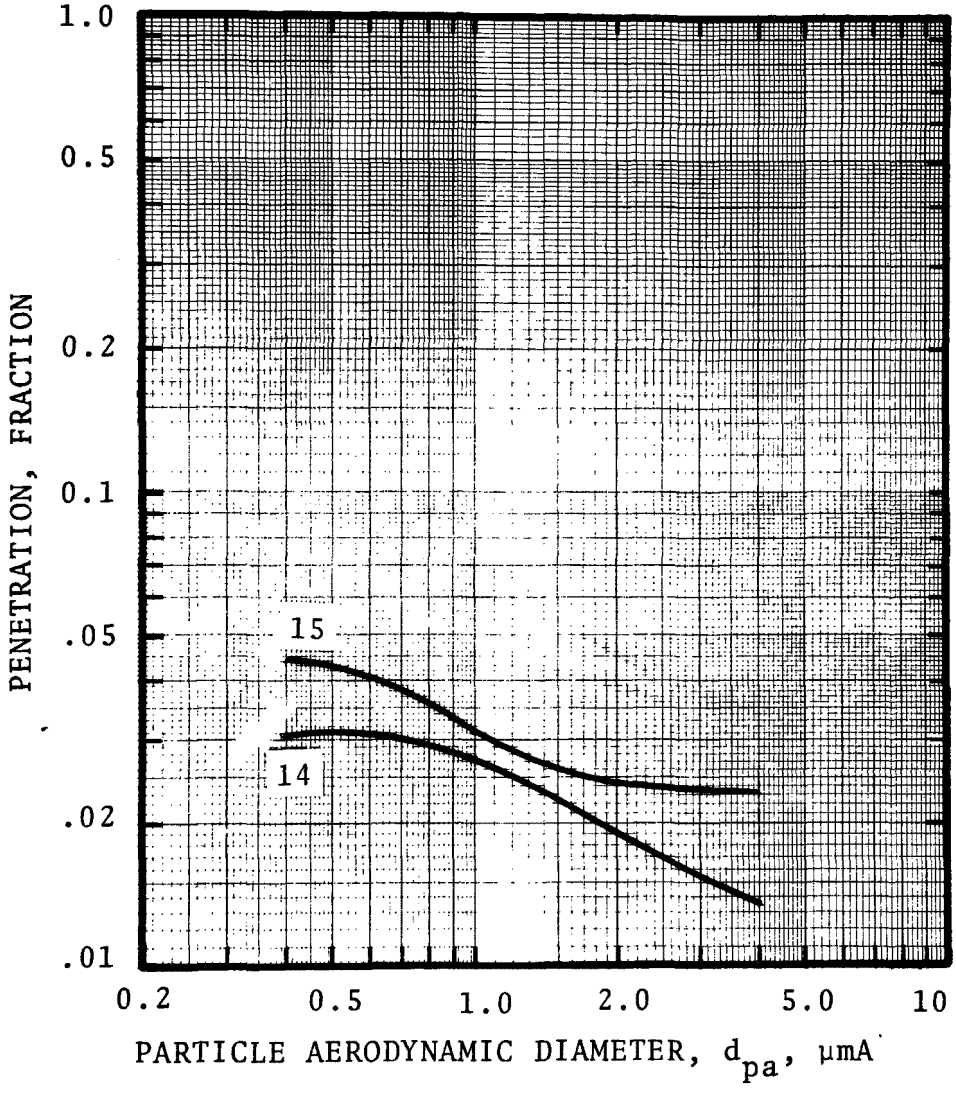

Figure 9. Particle penetration for cascade impactor runs 14 and 15.

SECTION 9

OPERATING PROBLEMS

The primary operating problem with the system at first was the limiting capacity of the fan. Great amounts of excess air were getting into the system through all of the leaks, resulting in the fan running at its maximum capacity. Because of this factor the system could not pull enough gas through the scrubber and a large portion exited through the top of the cupola. The amount of water that could be added to the system was also limited which in turn affected the scrubber efficiency.

Once most of these leaks were patched, however, the fan amperage dropped well below the limit, and the system could be adjusted easily.

The scrubber liquor was another operational problem. Since the cyclone entrainment separator was not working effectively, much of the water used to capture the particles was carried over and through the fan and out the stack. The scrubber liquor was recycled and changed only at the end of each day, which meant that the solids concentration increased as the day progressed. Reentrainment of this water, therefore, would mean higher outlet loadings since this extra weight was considered in the emission rates.

Corrosion had a severe effect on the system operation since it was the cause of the excessive leakage of air into the scrubber and entrainment separator.

Another problem with the system was the absence of a cap on the cupola top. This allowed the gases to escape through the top. Not all the gases pass through the scrubber and

therefore are not treated effectively, which in turn caused a visible emission problem. This can be alleviated by capping the cupola top.

SECTION 10

ECONOMICS

The scrubber system was built about ten years ago with substantial participation by the foundry. Consequently, the cost was distributed among several purchased components, contracted work, and foundry performed work. Records of the costs were not kept.

The operating cost for the blower (300 kW motor) was about $72.00 per day, based on eight hours use per day.

SECTION 11

PERFORMANCE COMPARISON

The performance of venturi-type scrubbers has been modeled extensively. A recent survey and the model used here are presented in Yung, et al. (1977) which is summarized in Appendix "C".

The scrubber parameters are known or estimated from the average of the conditions for the sets of runs shown in Table 8. The velocity attained by the liquid drops at the throat exit is often as high as 80% of the gas velocity. However, the pressure drop predicted based on this velocity accommodation is much higher than measured. The model predicts that the throat length for this 80% velocity attainment by drops should have been about 0.8 m. Since the actual throat length was only about 0.1 m the lower measured pressure drop is reasonable. For a throat length of 0.1 m the drops attain only about 60% of the gas velocity for most of the runs according to the model. And the predicted pressure drops more closely match those measured.

The predicted particle penetrations are shown compared to the average of the run sets in Figures 10-14. The solid (measurement) curves represent the measured penetration without accounting for leakage. The dashed curves assume that the outlet was diluted by the factor listed in Table 8 which is based on the data in Table 2. Table 9 presents the predicted pressure drop for a 0.1 m throat length and the overall penetration for d_{pg} = 0.4 μmA, σ_g = 2.5. These values may be compared to the measured values, presented in Tables 7 and 8.

The comparison of predicted and measured penetration leads to the following observations:

1. The predictions are generally close to the experimental results for particles around 1 μmA diameter. Runs 5, 6, and 7

TABLE 8. AVERAGE CONDITIONS FOR PERFORMANCE PREDICTIONS

Run Set	ΔP cm W.C.	Q_G m^3/s	Q_L/Q_G m^3/m^3	u_t m/s	T_G °C	ρ_G kg/m^3	μ_G kg/m-s	Dil*
5,6,7	79	11.1	0.0011	106	168	0.72	2.1×10^{-5}	1.23
8	83	10.8	0.0009	232	177	0.70	2.2×10^{-5}	1.27
9,10	82	12.5	0.0008	244	688	0.36	4.1×10^{-5}	1.88
11,12,13	103	4.1	0.0031	104	66	0.93	1.7×10^{-5}	1.79
14,15	88	9.8	0.0016	104	122	0.80	2.0×10^{-5}	1.22

*"Dil" is the ratio of measured outlet to inlet volume flow rates at standard conditions.

TABLE 9. PREDICTED PRESSURE DROP AND OVERALL PENETRATION

Run Set	ΔP cm W.C.	Penetration %
5,6,7	78	47
8	349	26
9,10	342	33
11,12,13	148	44
14,15	91	45

Assumptions: Throat Length = 0.1 m

d_{pg} = 0.4 μmA

σ_g = 2.5

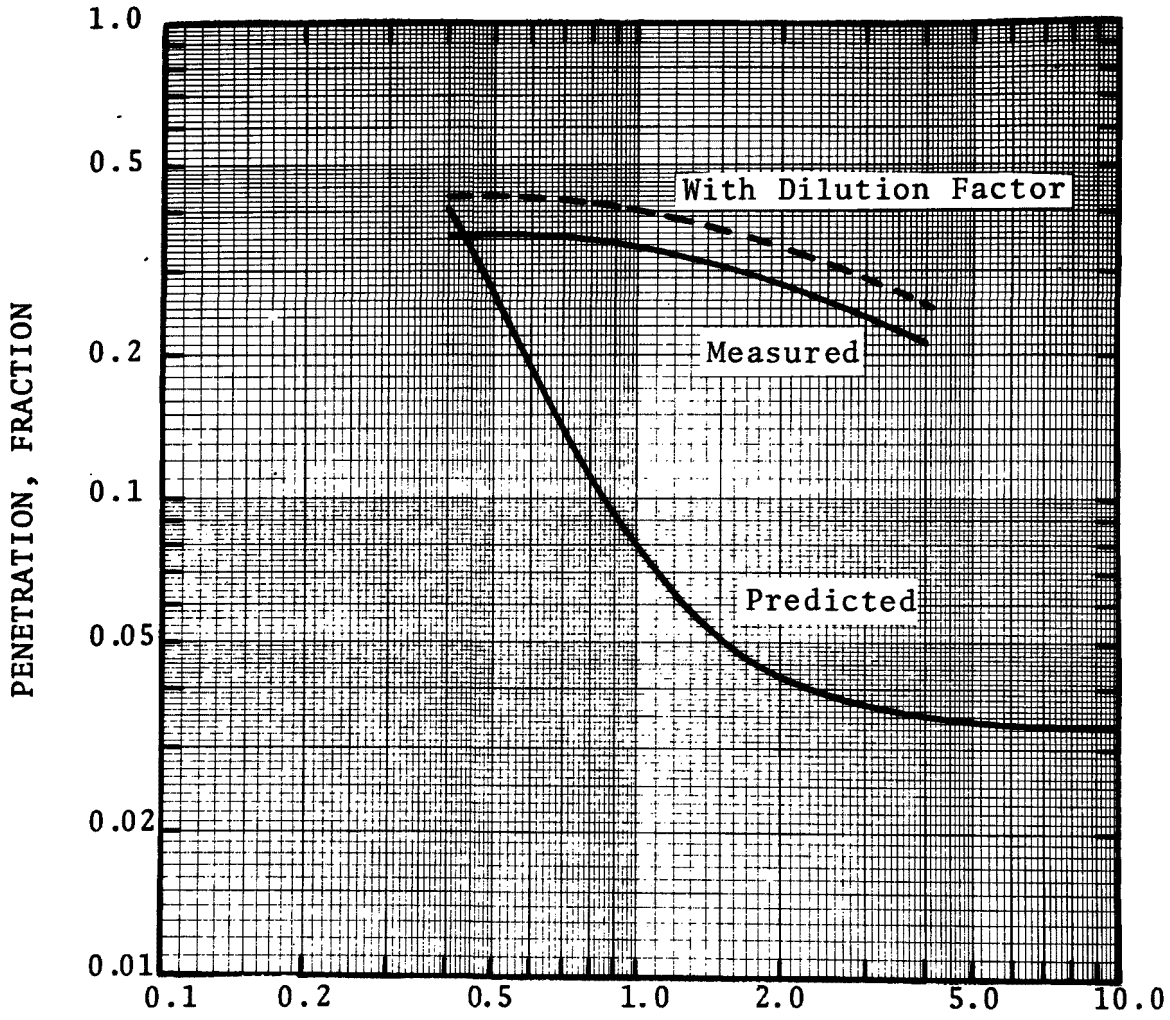

Figure 10. Comparison of predicted with measured penetration for average of Runs 5, 6, and 7.

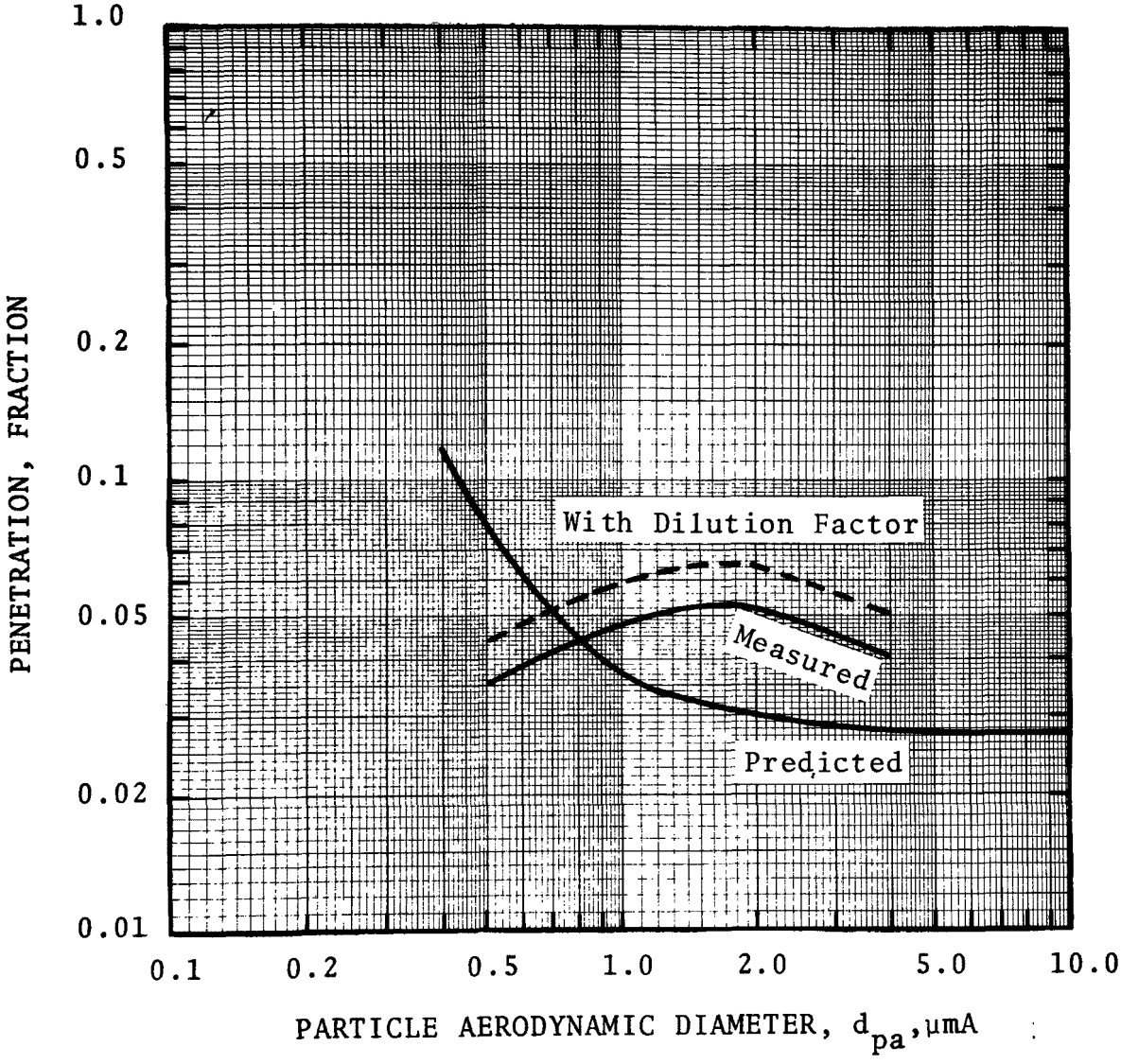

Figure 11. Comparison of predicted with measured penetration for Run 8.

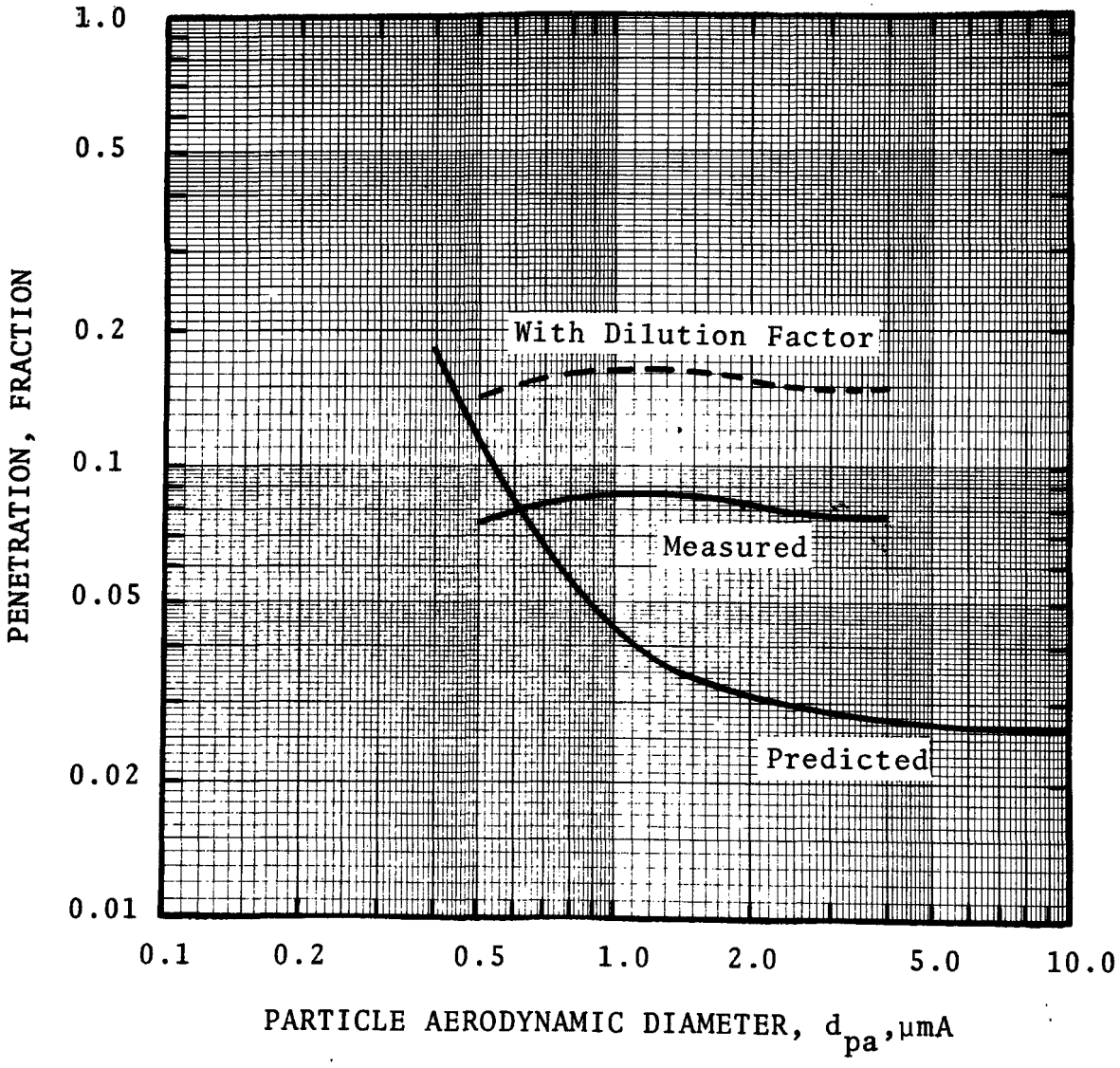

Figure 12. Comparison of predicted with measured penetration for average of Runs 9 and 10.

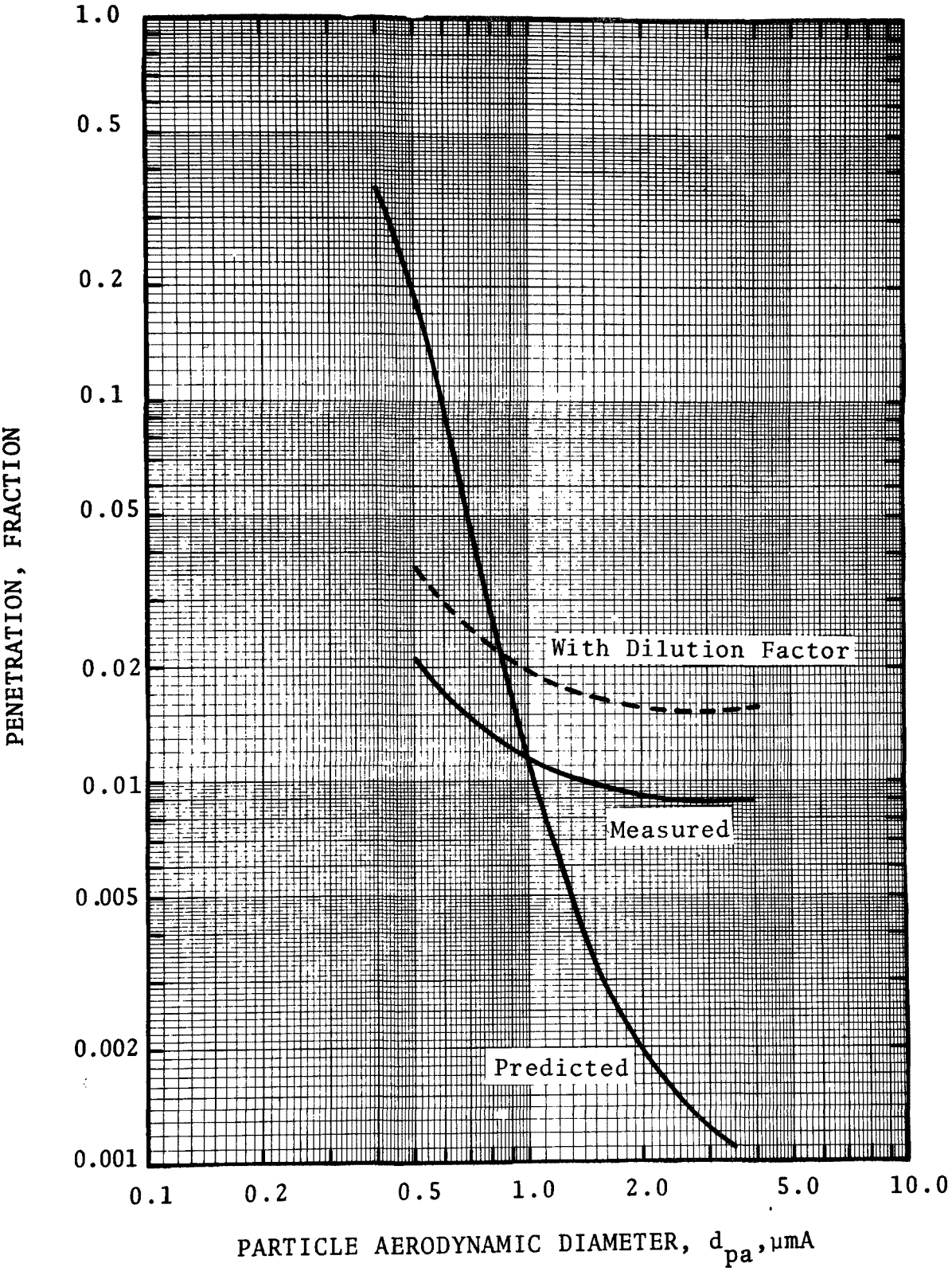

Figure 13. Comparison of predicted with measured penetration for average of Runs 11, 12, and 13.

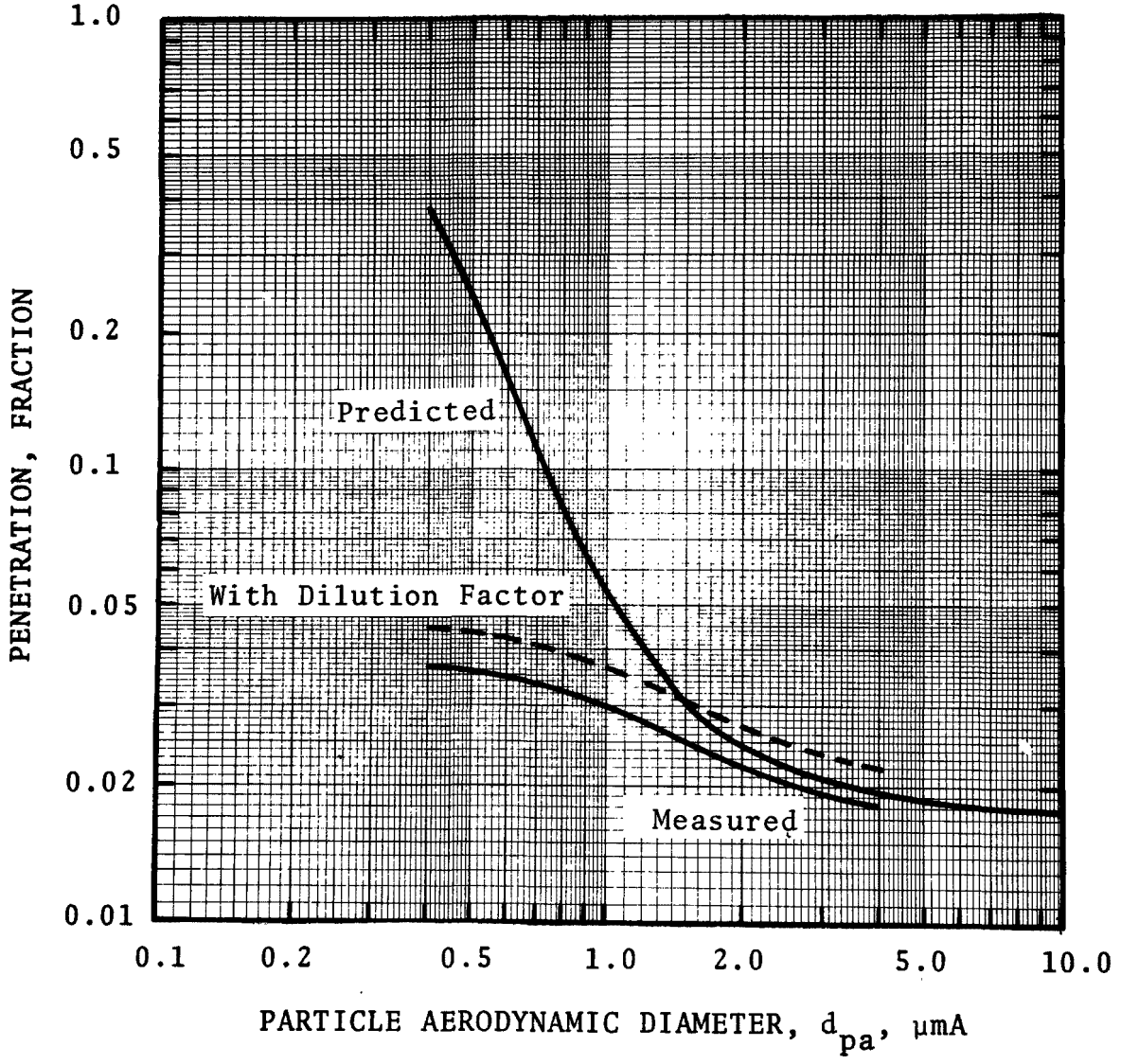

Figure 14. Comparison of predicted with measured penetration for average of Runs 14 and 15.

have the poorest fit. Although the operating conditions for these runs were similar to those of runs 14 and 15, the experimental penetration was greater. This may be due to the fact that the gas flow rate was higher in runs 5, 6, and 7 which could mean more leakage and could cause more entrainment carryover at the outlet. The effect of L/G ratio on the model predictions is shown by comparing the predicted penetrations of these two run sets. The main difference in the operating conditions was that runs 14 and 15 had a 45% higher L/G ratio than runs 5, 6, and 7.

2. Predicted penetration for sub-micron particles is generally higher than measured. This may be due to condensation caused by the cool duct walls and the cool scrubber liquid which had low temperatures due to the cold ambient air (0°C). Leaks of the cold ambient air into the system would also have caused condensation.

3. Predicted penetration is generally lower than measured for particles larger than about 1 μmA diameter. There are several plausible causes of this disparity:

a. Entrainment not collected in the entrainment separator would yield particles in the larger size range. The cyclone separator was known to be inefficient although its performance was improved by internal modifications and leak patching. This inefficiency was clearly demonstrated by noticeable liquid drops at the outlet stack where the sampling crew was working, and by the pre-cutter mass collections.

b. Imprecise knowledge of the liquid flow rate can cause the prediction to be substantially incorrect in the larger particle size range. This effect becomes more serious as the liquid/gas ratio decreases, as seen by comparing the prediction of runs 5, 6, and 7 with that of runs 14 and 15.

4. Predicted overall penetration was generally higher than measured. This difference is probably due primarily to the assumption that the size distribution is log-normal with the same standard deviation for all particles less than 0.4 μmA (d_{pg}).

Condensation probably affected the log-normality of the small size distribution. Also, the penetration model over-predicted the penetration of the smaller particles which would definitely cause the overall penetration prediction to be too high.

In conclusion, with all the real effects considered, the model provides an adequate prediction. Predictions for several of the runs, notably 8, 11, 12, 13, 14, and 15, were quite good.

REFERENCES

Lipson, C., and N.J. Sheth, "Statistical Design and Analysis of Engineering Experiments," McGraw-Hill, 1973.

Raabe, O.G., "Aerosol Aerodynamic Size Conventions for Inertial Sampler Calibration," J. Air Poll. Control Assoc., 26:856-860, 1976.

Yung, S., S. Calvert, and H.F. Barbarika, "Venturi Scrubber Performance Model," A.P.T., Inc., San Diego, California. EPA Contract No. 68-02-1328, Task No. 13, July 1977.

APPENDIX A

Cascade Impactor Data

TABLE A-1. INLET AND OUTLET SAMPLE PARTICLE DATA FOR RUN #1

IMPACTOR STAGE NUMBER	INLET		OUTLET	
	M_{cum} (mg/DNm^3)	d_{pc} (μmA)	M_{cum} (mg/DNm^3)	d_{pc} (μmA)
Precutter & Nozzle	1,570	12.40	212.0	6.57
1	1,360	46.80	46.3	25.0
2	1,360	3.98	43.6	11.0
3	1,360	2.28	41.3	5.19
4	1,320	1.27	41.3	2.12
5	1,260	0.76	37.4	1.22
6	862	0.42	30.5	0.67
7	556	0.23	20.8	0.40
Filter	375		6.2	
Sample Volume (DNm^3)	0.070		0.260	

M_{cum} = cumulative mass collected on that stage and those below

d_{pc} = cut diameter (aerodynamic) for that stage

μmA = microns, aerodynamic = $d_p(C' \rho_p)^{1/2}$

d_p = particle diameter (actual)

C' = Cunningham correction factor

ρ_p = particle density (g/cm^3)

DNm^3 = dry normal cubic meters (0°C, 1 atm)

TABLE A-2. INLET AND OUTLET SAMPLE PARTICLE DATA FOR RUN #2

IMPACTOR STAGE NUMBER	INLET		OUTLET	
	M_{cum} (mg/DNm³)	d_{pc} (μmA)	M_{cum} (mg/DNm³)	d_{pc} (μmA)
Precutter & Nozzle	2,120	12.1	74.3	6.35
1	1,800	45.4	36.5	24.90
2	1,770	3.86	35.9	10.90
3	1,750	2.21	35.9	4.21
4	1,710	1.23	34.2	2.11
5	1,630	0.71	27.4	1.21
6	1,090	0.40	22.3	0.67
7		0.22	17.5	0.38
Filter	530		11.9	
Sample Volume (DNm³)	0.030		0.520	

TABLE A-3. INLET AND OUTLET SAMPLE PARTICLE DATA FOR RUN #3

IMPACTOR STAGE NUMBER	INLET		OUTLET	
	M_{cum} (mg/DNm³)	d_{pc} (μmA)	M_{cum} (mg/DNm³)	d_{pc} (μmA)
Precutter & Nozzle	1,100	11.70	280	5.41
1	833	43.80	267	21.20
2	833	3.73	267	9.30
3	833	2.14	266	3.97
4	824	1.19	264	1.80
5	790	0.71	256	1.03
6	652	0.39	238	0.57
7	357	0.21	187	0.33
Filter	219		116	
Sample Volume (DNm³)	0.020		0.380	

TABLE A-4. INLET AND OUTLET SAMPLE PARTICLE DATA FOR RUN #4

IMPACTOR STAGE NUMBER	INLET		OUTLET	
	M_{cum} (mg/DNm³)	d_{pc} (μmA)	M_{cum} (mg/DNm³)	d_{pc} (μmA)
Precutter & Nozzle	2,060	11.40	176	5.84
1	1,710	42.80	175	22.30
2	1,710	3.64	174	9.76
3	1,700	2.09	171	3.77
4	1,680	1.16	162	1.89
5	1,630	0.67	143	1.08
6	1,460	0.38	91.7	0.60
7	936	0.20	47.4	0.34
Filter	691			
Sample Volume (DNm³)	0.020		0.610	

TABLE A-5. INLET AND OUTLET SAMPLE PARTICLE DATA FOR RUN #5

IMPACTOR STAGE NUMBER	INLET		OUTLET	
	M_{cum} (mg/DNm³)	d_{pc} (μmA)	M_{cum} (mg/DNm³)	d_{pc} (μmA)
Precutter & Nozzle	3,190	10.10	609	5.47
1	1,570	38.00	514	21.0
2	1,570	3.23	513	9.20
3	1,550	1.85	511	4.36
4	1,520	1.03	506	1.78
5	1,470	0.62	490	1.02
6	1,350	0.33	466	0.56
7	1,000	0.18	365	0.33
Filter	800		238	
Sample Volume (DNm³)	0.020		0.200	

TABLE A-6. INLET AND OUTLET SAMPLE PARTICLE DATA FOR RUN #6

IMPACTOR STAGE NUMBER	INLET		OUTLET	
	M_{cum} (mg/DNm³)	d_{pc} (μmA)	M_{cum} (mg/DNm³)	d_{pc} (μmA)
Precutter & Nozzle	2,340	10.10	341	5.47
1	1,250	38.10	307	21.10
2	1,250	3.24	306	9.24
3	1,250	1.86	305	3.57
4	1,230	1.03	299	1.79
5	1,190	0.59	287	1.02
6	1,050	0.34	268	0.57
7	577	0.18	205	0.32
Filter	269		112	
Sample Volume (DNm³)	0.010		0.300	

TABLE A-7. INLET AND OUTLET SAMPLE PARTICLE DATA FOR RUN #7

IMPACTOR STAGE NUMBER	INLET		OUTLET	
	M_{cum} (mg/DNm³)	d_{pc} (μmA)	M_{cum} (mg/DNm³)	d_{pc} (μmA)
Precutter & Nozzle	2,530	10.50	234	5.21
1	1,460	39.60	234	20.20
2	1,450	3.37	233	8.85
3	1,430	1.93	232	3.42
4	1,410	1.07	227	1.72
5	1,360	0.62	218	0.98
6	1,190	0.35	202	0.54
7	627	0.19	156	0.30
Filter	246		81.8	
Sample Volume (DNm³)	0.010		0.350	

TABLE A-8. INLET AND OUTLET SAMPLE PARTICLE DATA FOR RUN #8

IMPACTOR STAGE NUMBER	INLET		OUTLET	
	M_{cum} (mg/DNm³)	d_{pc} (μmA)	M_{cum} (mg/DNm³)	d_{pc} (μmA)
Precutter & Nozzle	1,910	10.40	320	5.72
1	1,850	39.20	98.2	22.10
2	1,850	3.33	96.7	9.67
3	1,840	1.91	96.4	4.58
4	1,810	1.06	95.0	1.87
5	1,720	0.64	90.8	1.07
6	1,260	0.35	84.7	0.59
7	559	0.18	71.6	0.35
Filter	236		45.8	
Sample Volume (DNm³)	0.020		0.670	

TABLE A-9. INLET AND OUTLET SAMPLE PARTICLE DATA FOR RUN #9

IMPACTOR STAGE NUMBER	INLET		OUTLET	
	M_{cum} (mg/DNm³)	d_{pc} (μmA)	M_{cum} (mg/DNm³)	d_{pc} (μmA)
Precutter & Nozzle	5,070	16.10	198	5.69
1	1,510	60.50	156	20.70
2	1,490	5.15	156	9.07
3	1,480	2.95	154	4.30
4	1,430	1.64	151	1.76
5	1,380	0.99	142	1.01
6	1,230	0.54	129	0.56
7	648	0.31	90.7	0.33
Filter	267		48.2	
Sample Volume (DNm³)	0.020		0.520	

TABLE A-10. INLET AND OUTLET SAMPLE PARTICLE DATA FOR RUN #10

IMPACTOR STAGE NUMBER	INLET		OUTLET	
	M_{cum} (mg/DNm³)	d_{pc} (μmA)	M_{cum} (mg/DNm³)	d_{pc} (μmA)
Precutter & Nozzle	2,620	14.40	589	5.31
1	1,740	54.20	159	20.50
2	1,710	4.61	157	8.96
3	1,680	2.64	156	3.46
4	1,660	1.47	153	1.74
5	1,590	0.85	146	0.99
6	1,460	0.48	135	0.55
7	1,050	0.27	112	0.31
Filter	652		68.8	
Sample Volume (DNm³)	0.030		0.440	

TABLE A-11. INLET AND OUTLET SAMPLE PARTICLE DATA FOR RUN #11

IMPACTOR STAGE NUMBER	INLET		OUTLET	
	M_{cum} (mg/DNm³)	d_{pc} (μmA)	M_{cum} (mg/DNm³)	d_{pc} (μmA)
Precutter & Nozzle	1,750	12.0	159	5.64
1	1,270	45.0	153	22.40
2	1,270	3.82	152	9.82
3	1,250	2.19	151	4.65
4	1,230	1.22	148	1.90
5	1,180	0.73	143	1.09
6	942	0.40	132	0.60
7	563	0.22	87.5	0.36
Filter	388		45.5	
Sample Volume (DNm³)	0.020		0.570	

TABLE A-12. INLET AND OUTLET SAMPLE PARTICLE DATA FOR RUN #12

IMPACTOR STAGE NUMBER	INLET		OUTLET	
	M_{cum} (mg/DNm³)	d_{pc} (μmA)	M_{cum} (mg/DNm³)	d_{pc} (μmA)
Precutter & Nozzle	2,370	11.70	214	5.68
1	1,610	43.90	159	21.60
2	1,600	3.73	158	9.48
3	1,570	2.14	158	3.66
4	1,540	1.19	155	1.84
5	1,450	0.68	145	1.05
6	1,270	0.39	132	0.58
7	711	0.21	103	0.33
Filter	404		61.0	
Sample Volume (DNm³)	0.030		0.620	

TABLE A-13. INLET AND OUTLET SAMPLE PARTICLE DATA FOR RUN #13

IMPACTOR STAGE NUMBER	INLET		OUTLET	
	M_{cum} (mg/DNm³)	d_{pc} (μmA)	M_{cum} (mg/DNm³)	d_{pc} (μmA)
Precutter & Nozzle	2,500	11.0	797	5.42
1	1,920	41.20	174	21.0
2	1,920	3.51	174	9.21
3	1,900	2.01	173	4.36
4	1,860	1.12	170	1.78
5	1,790	0.67	161	1.02
6	1,500	0.36	149	0.56
7	988	0.20	112	0.33
Filter	680		71.5	
Sample Volume (DNm³)	0.030		0.570	

TABLE A-14. INLET AND OUTLET SAMPLE PARTICLE DATA FOR RUN #14

IMPACTOR STAGE NUMBER	INLET		OUTLET	
	M_{cum} (mg/DNm^3)	d_{pc} (µmA)	M_{cum} (mg/DNm^3)	d_{pc} (µmA)
Precutter & Nozzle	1,450	10.20	278	5.43
1	1,300	38.40	186	20.40
2	1,290	3.27	185	8.92
3	1,260	1.87	183	3.44
4	1,200	1.04	180	1.73
5	1,130	0.60	171	0.99
6	1,056	0.34	156	0.54
7	760	0.18	118	0.31
Filter	531		59.8	
Sample Volume (DNm^3)	0.010		0.470	

TABLE A-15. INLET AND OUTLET SAMPLE PARTICLE DATA FOR RUN #15

IMPACTOR STAGE NUMBER	INLET		OUTLET	
	M_{cum} (mg/DNm^3)	d_{pc} (µmA)	M_{cum} (mg/DNm^3)	d_{pc} (µmA)
Precutter & Nozzle	1,240	11.90	277	5.33
1	1,240	44.80	223	20.20
2	1,210	3.81	221	8.84
3	1,200	2.18	218	4.19
4	1,180	1.21	213	1.71
5	1,140	0.73	202	0.98
6	1,040	0.40	184	0.54
7	794	0.21	127	0.32
Filter	713		65.0	
Sample Volume (DNm^3)	0.010		0.330	

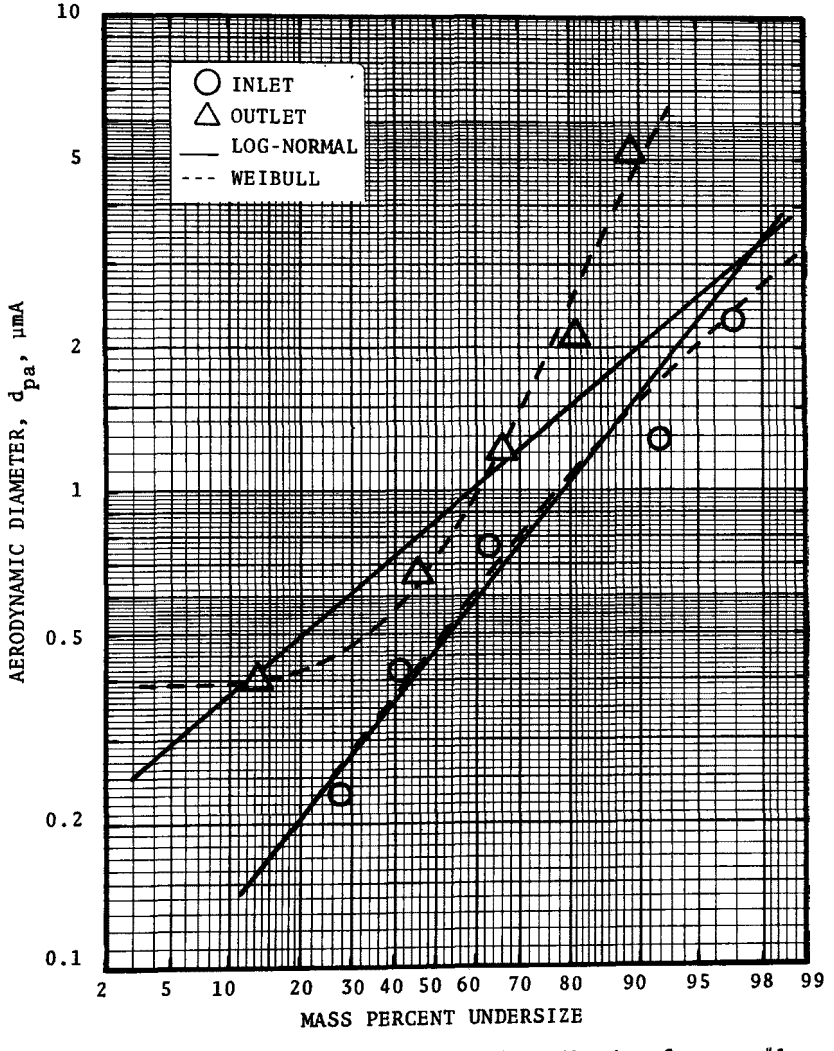

Figure A-1. Inlet and outlet size distribution for run #1.

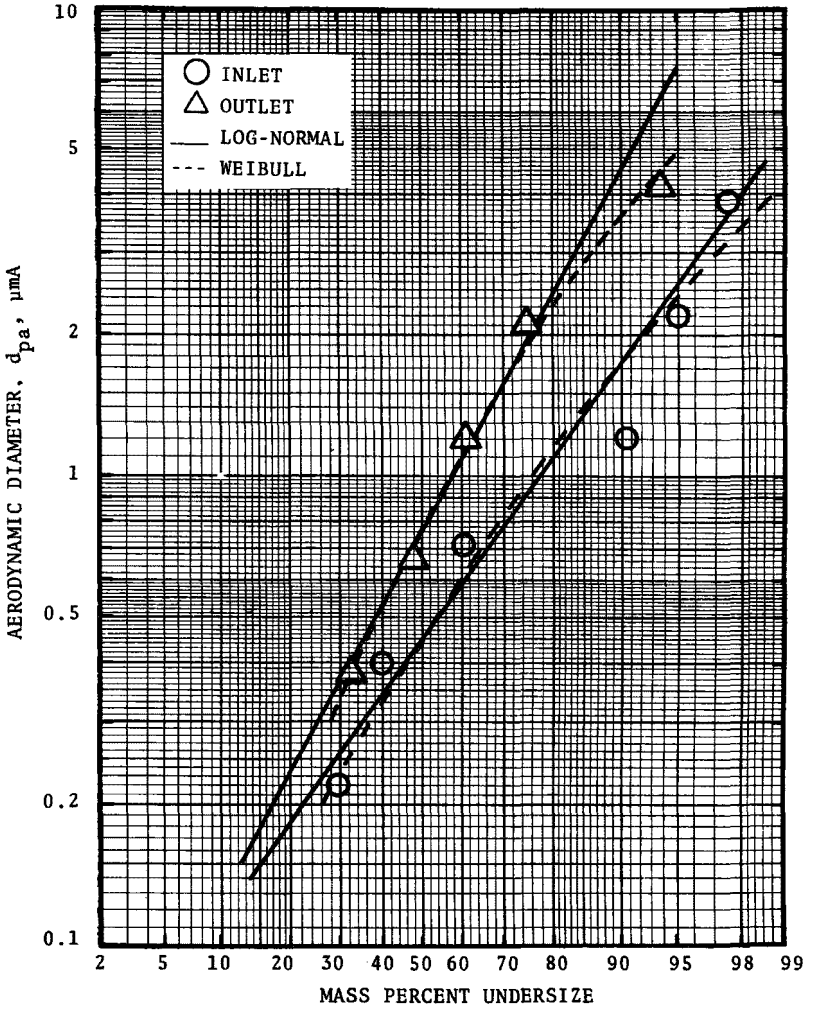

Figure A-2. Inlet and outlet size distribution for run #2.

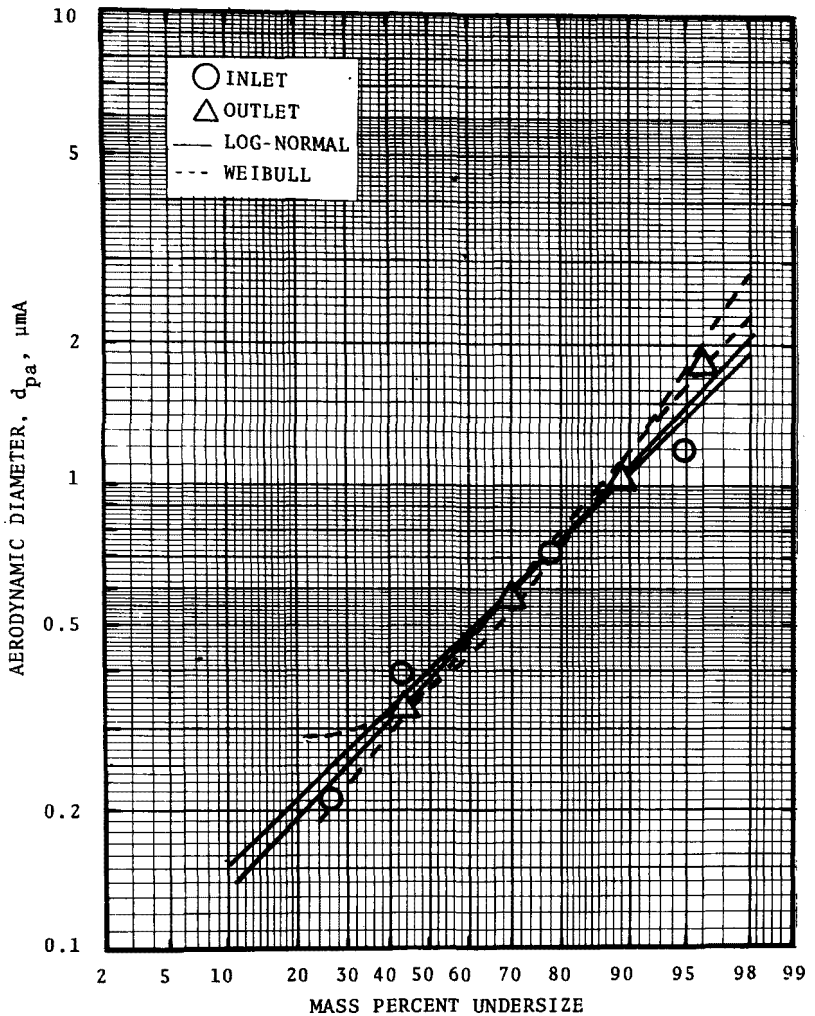

Figure A-3. Inlet and outlet size distribution for run #3.

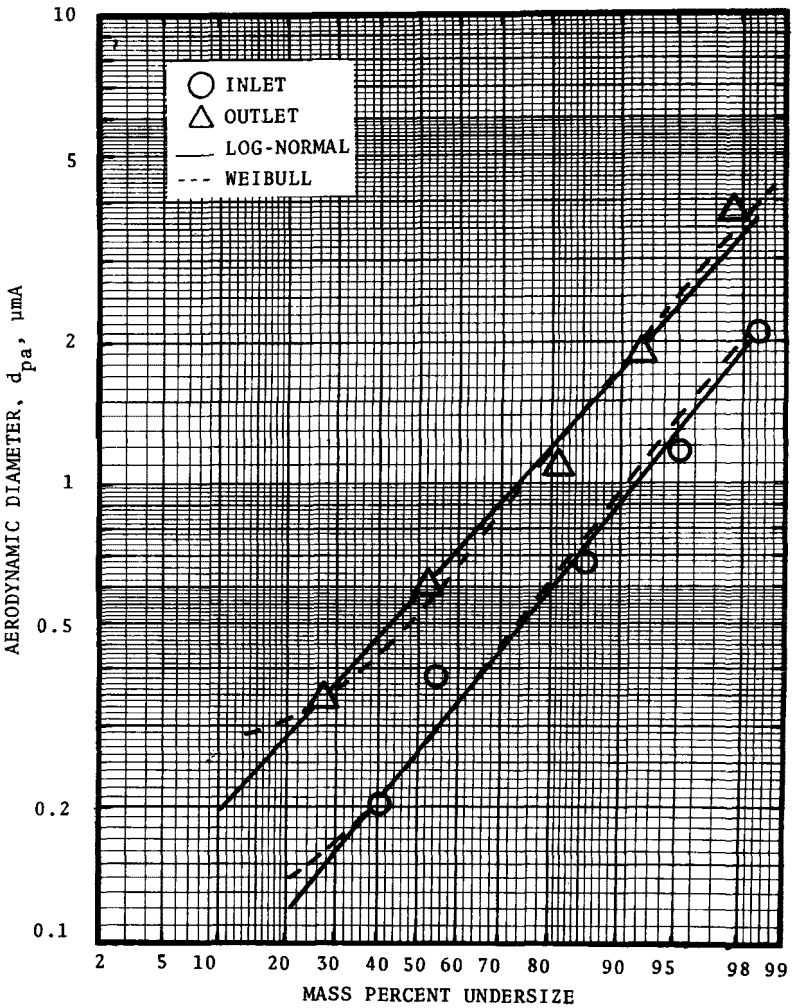

Figure A-4. Inlet and outlet size distribution for run #4.

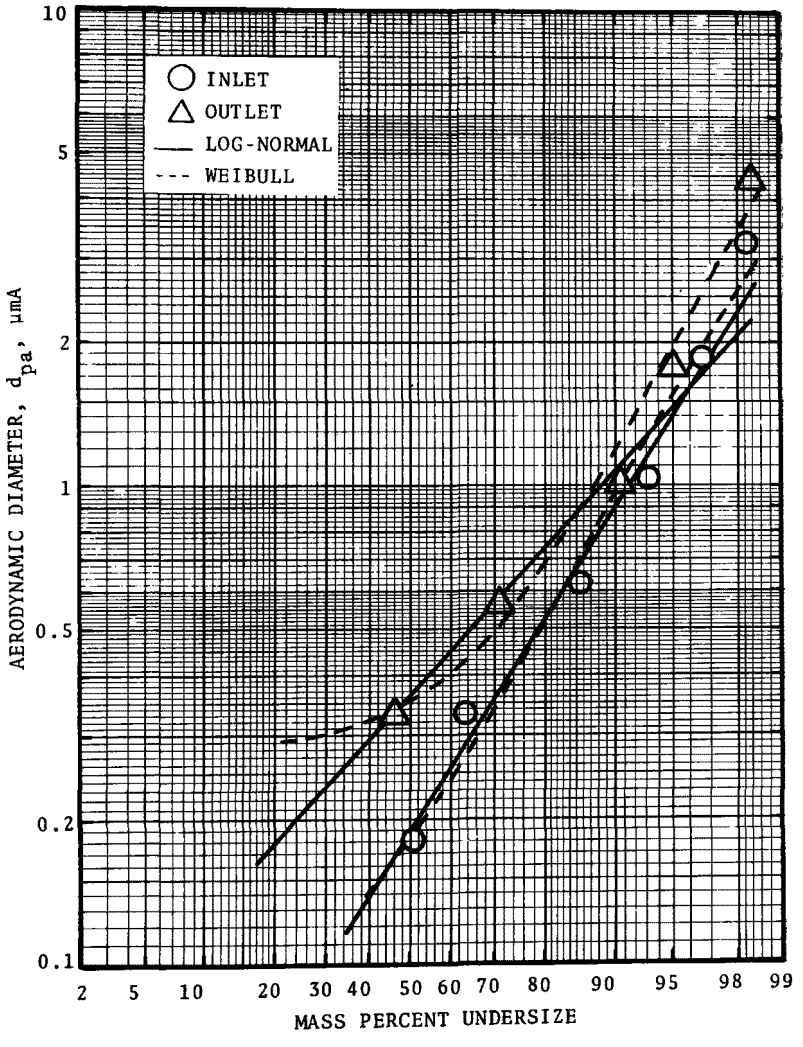

Figure A-5. Inlet and outlet size distribution for run #5.

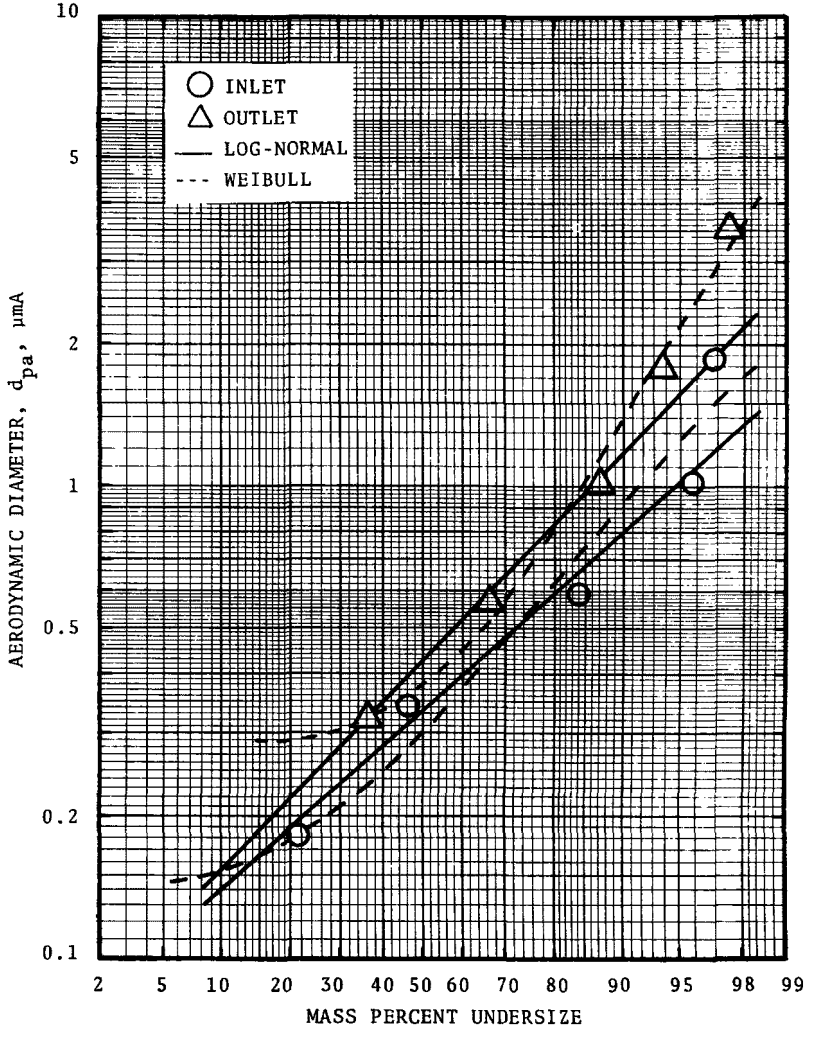

Figure A-6. Inlet and outlet size distribution for run #6.

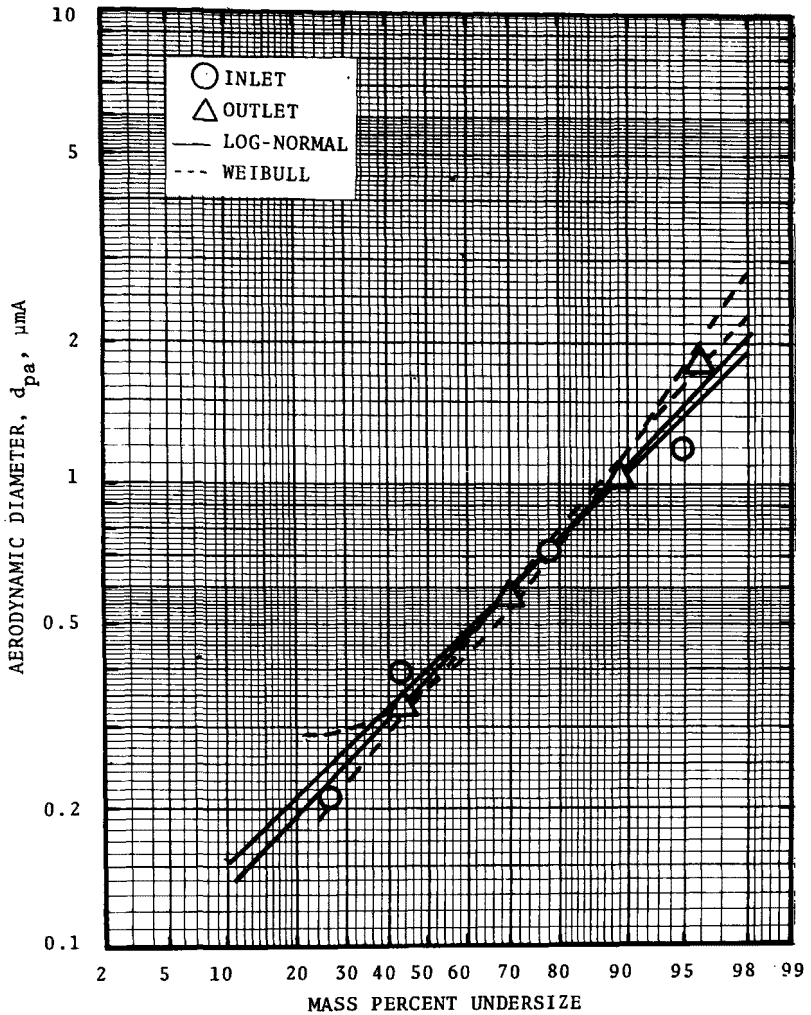

Figure A-3. Inlet and outlet size distribution for run #3.

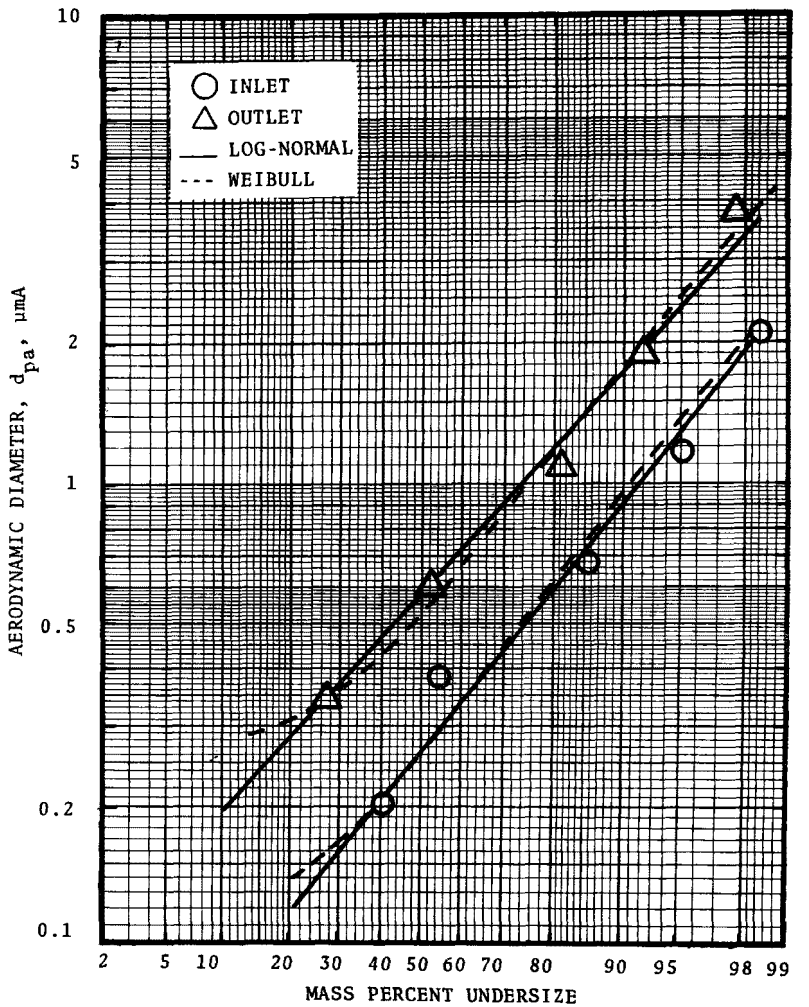

Figure A-4. Inlet and outlet size distribution for run #4.

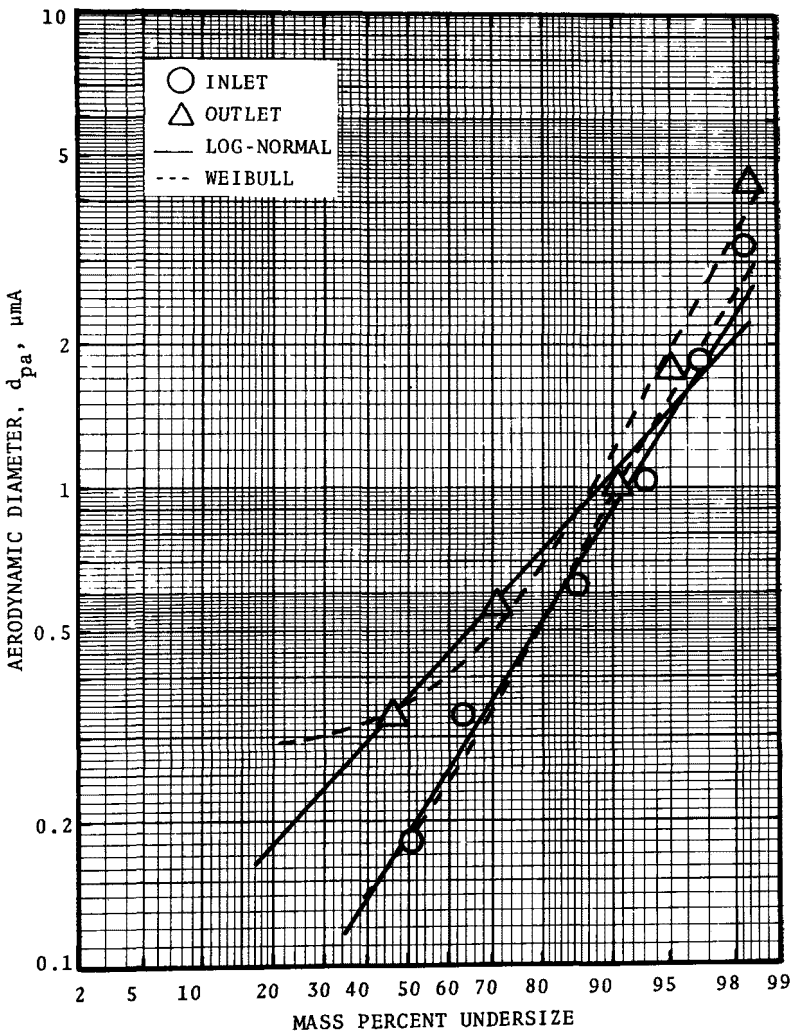

Figure A-5. Inlet and outlet size distribution for run #5.

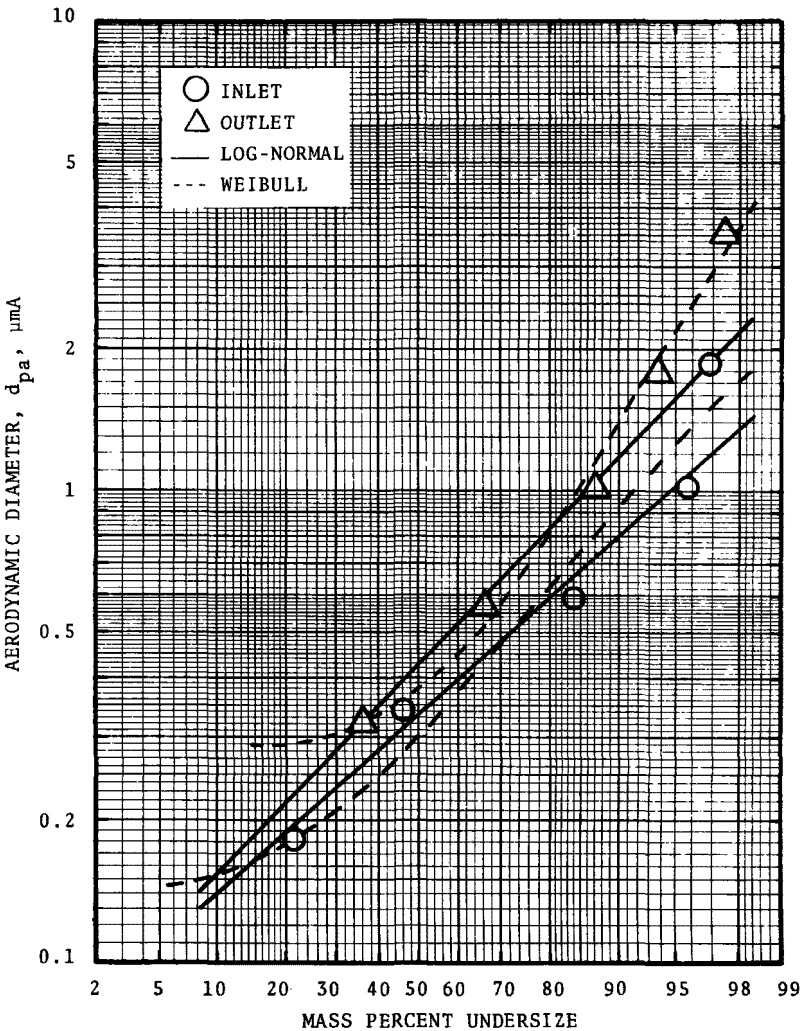

Figure A-6. Inlet and outlet size distribution for run #6.

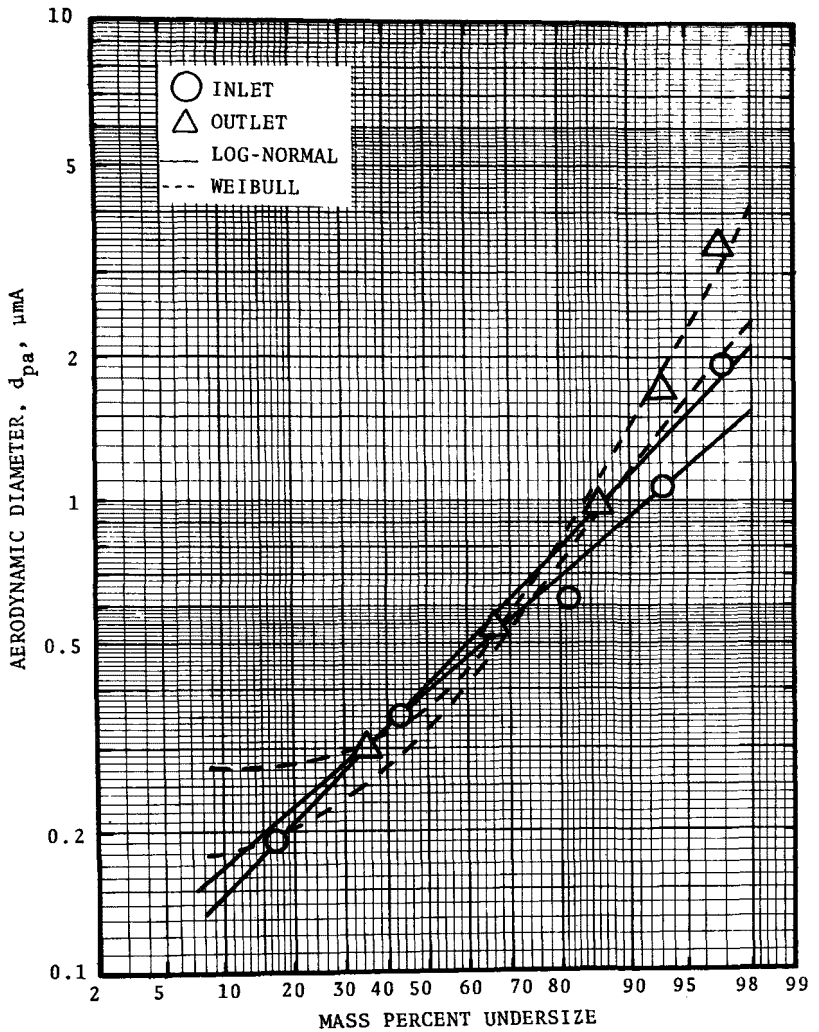

Figure A-7. Inlet and outlet size distribution for run #7.

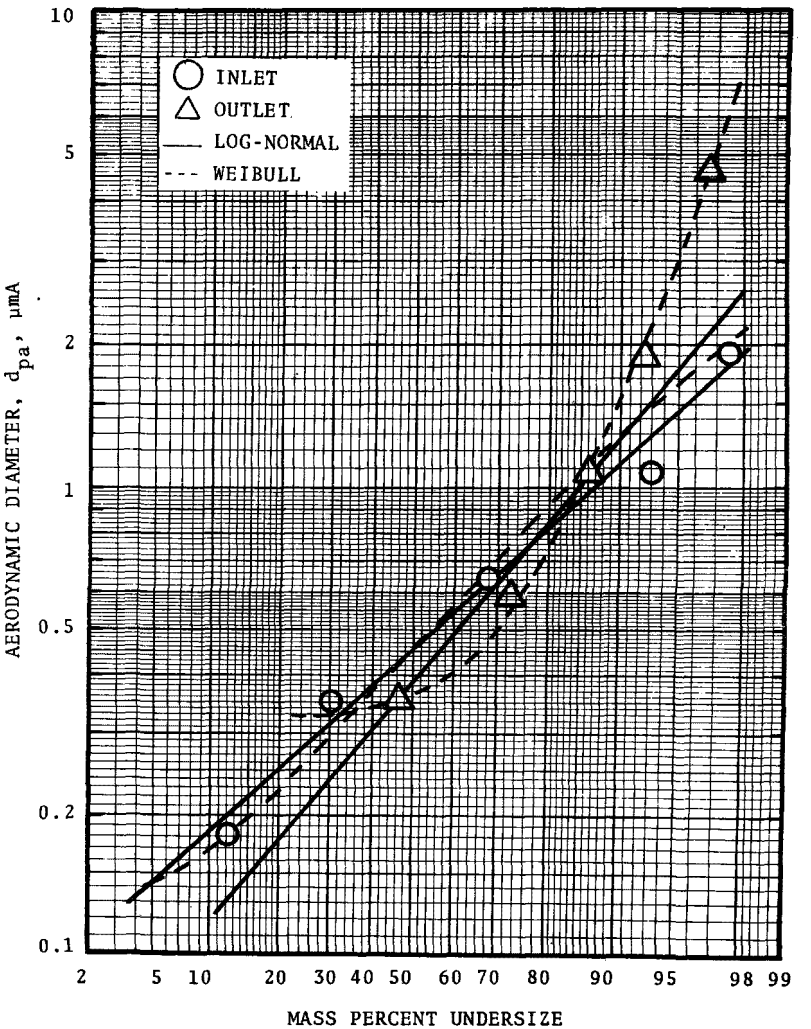

Figure A-8. Inlet and outlet size distribution for run #8.

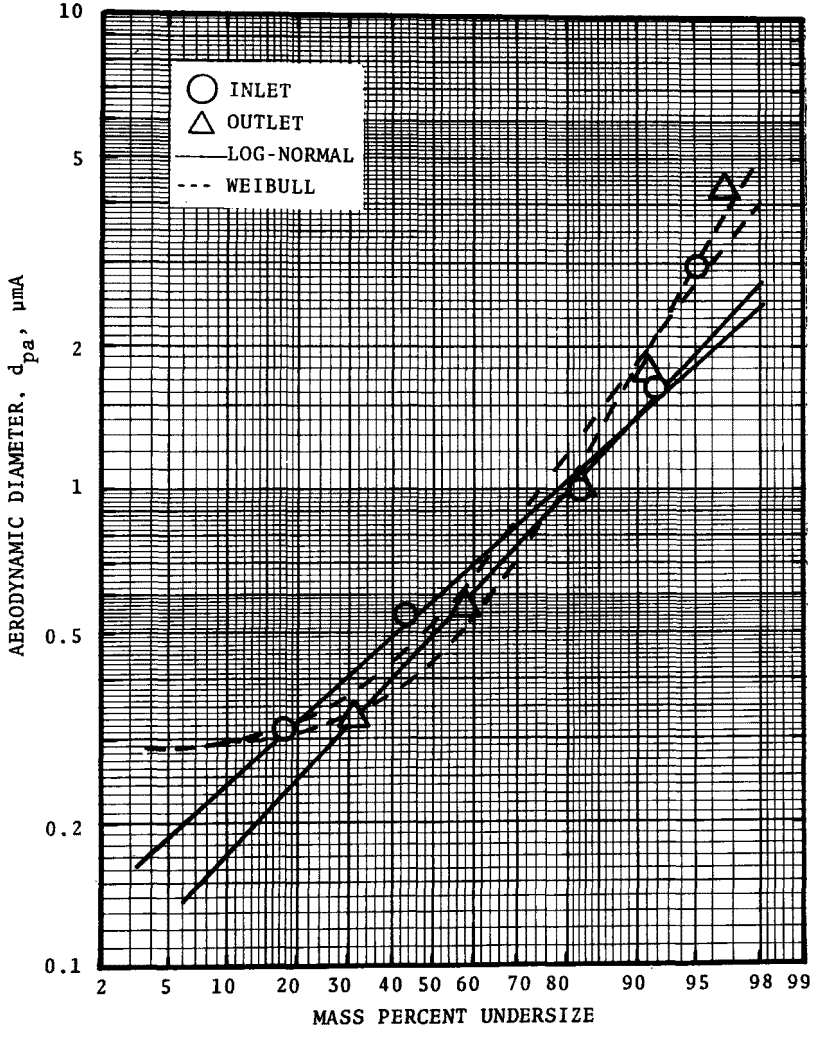

Figure A-9. Inlet and outlet size distribution for run #9.

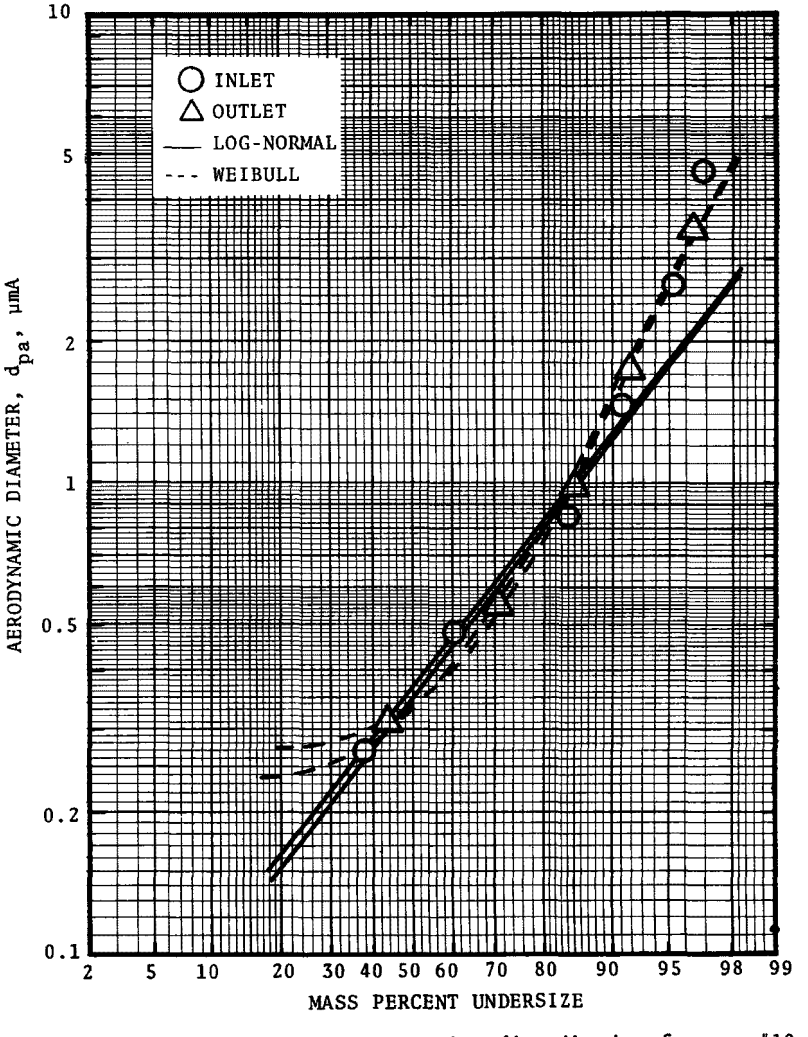

Figure A-10. Inlet and outlet size distribution for run #10.

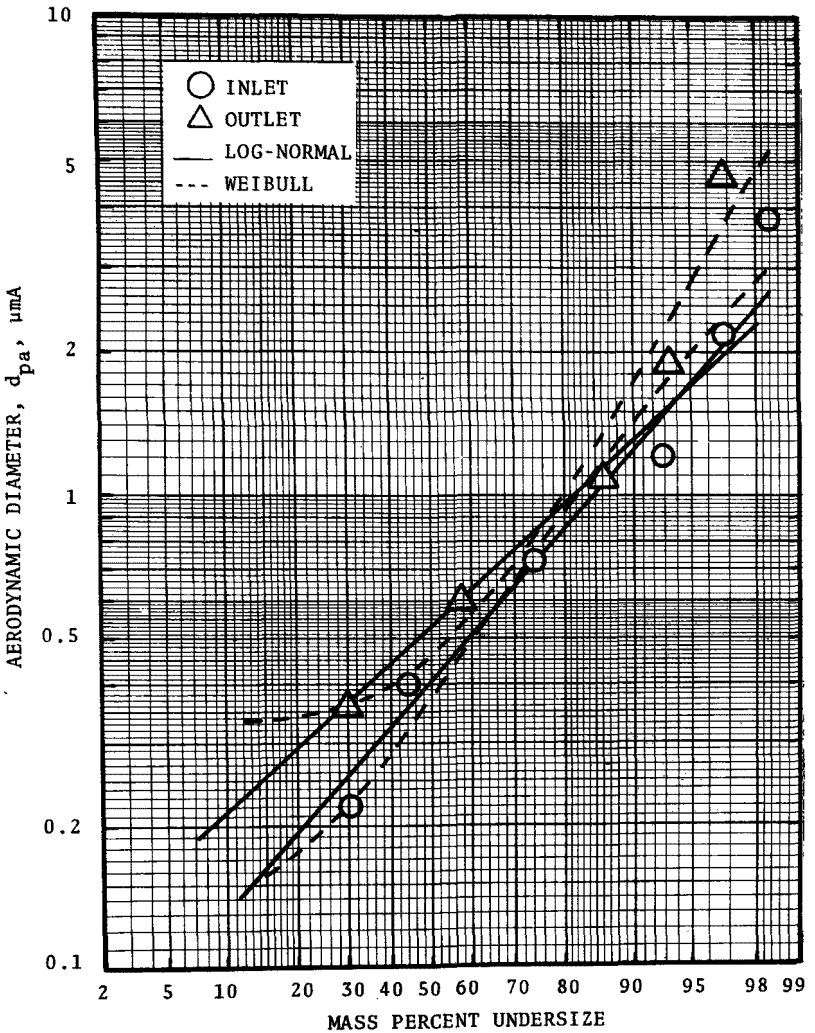

Figure A-11. Inlet and outlet size distribution for run #11.

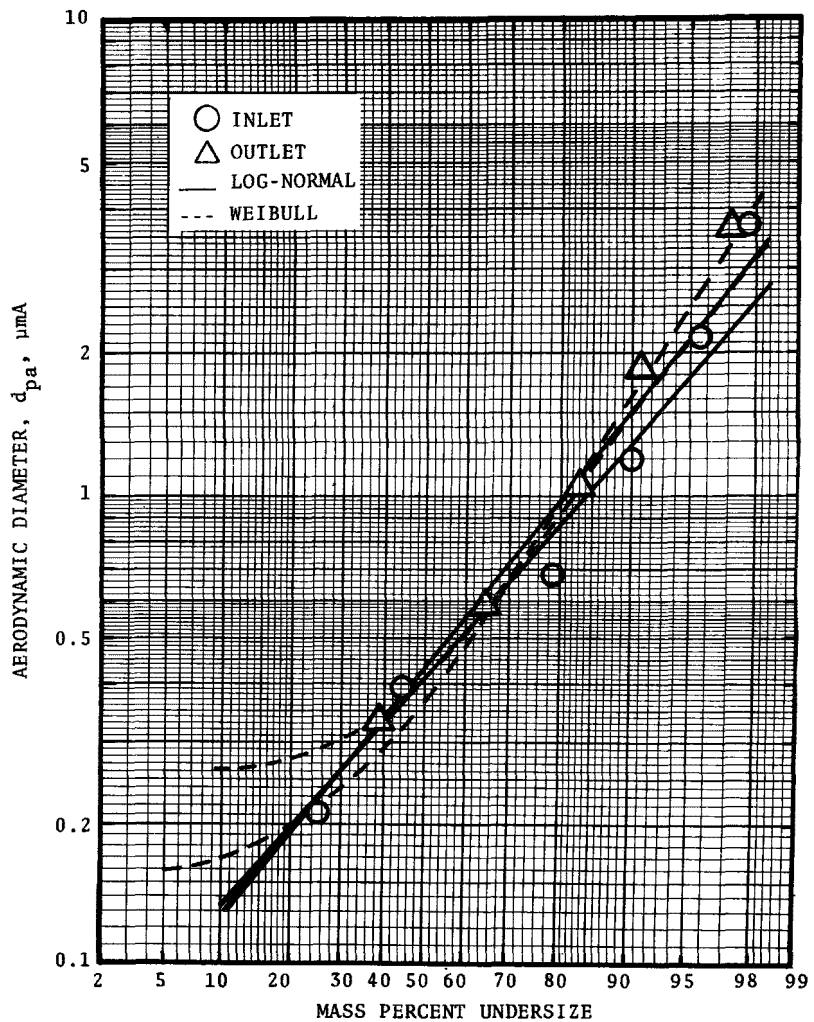

Figure A-12. Inlet and outlet size distribution for run #12.

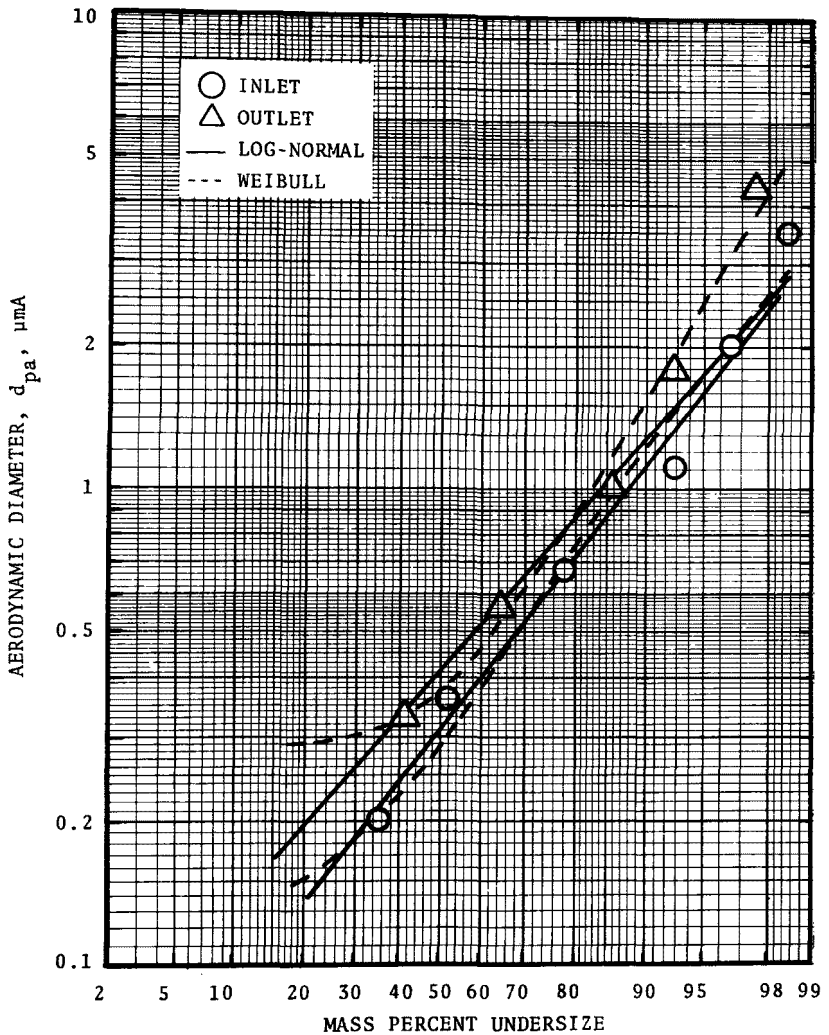

Figure A-13. Inlet and outlet size distribution for run #13.

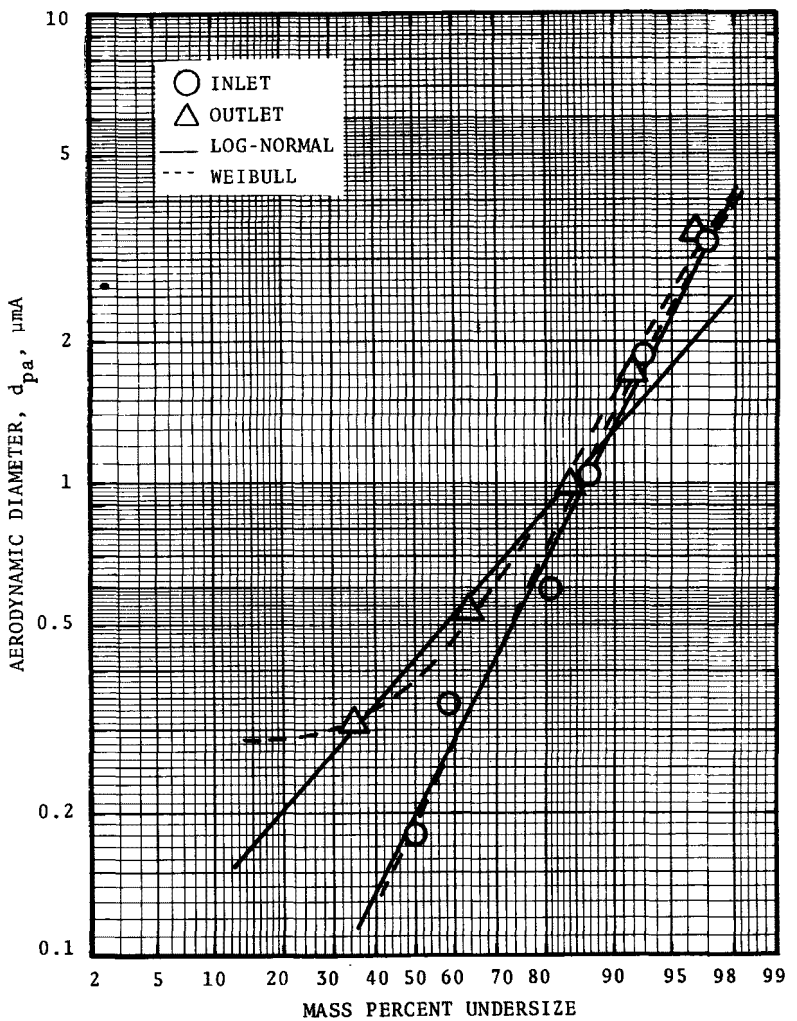

Figure A-14. Inlet and outlet size distribution for run #14.

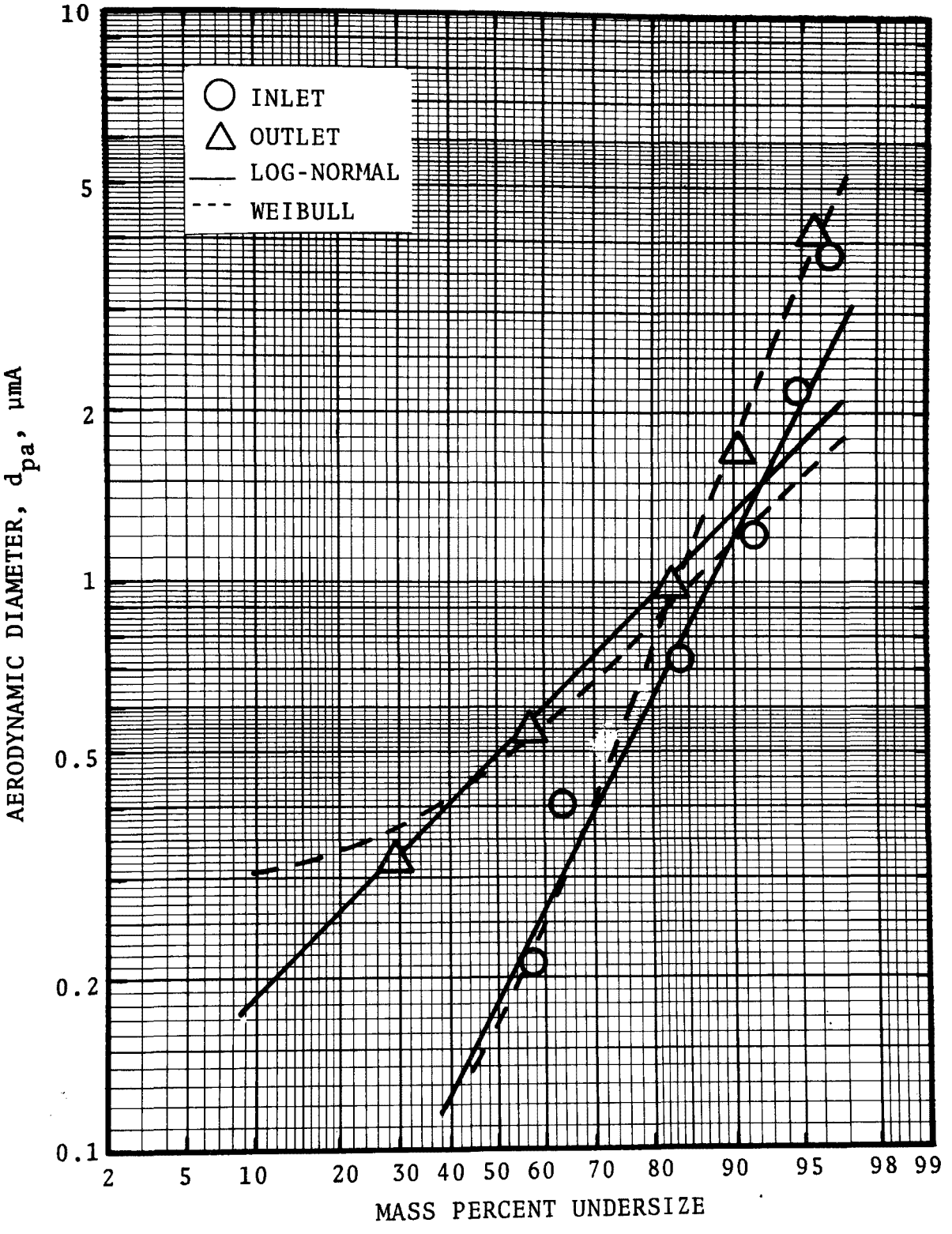

Figure A-15. Inlet and outlet size distribution for run #15.

APPENDIX B

Weibull Distribution

WEIBULL DISTRIBUTION

The Weibull distribution, Lipson (1973), offers two advantages over the log-probability distribution. The first is that it has three parameters rather than two. The second is that the cumulative distribution function (CDF) is explicit and does not have to be approximated by multi-termed polynomials.

Cumulative Distribution Function

$$CDF = 1 - \exp\left[- \left(\frac{d_p - d_{po}}{\Theta - d_{po}} \right)^b \right] \qquad \text{(B-1)}$$

where, d_p = particle diameter
d_{po} = minimum particle diameter
Θ = characteristic diameter
b = Weibull slope

The CDF has the property that:

$$CDF\ (\Theta = d_p) = 0.632$$

The median particle diameter occurs when the CDF = 0.5, so:

$$d_{pg} = d_{po} + (\Theta - d_{po})\ (\ln 2)^{1/b} \qquad \text{(B-2)}$$

Linear Transformation

Transformation to a linear form;

$$y = A + B\ x \qquad \text{(B-3)}$$

requires that:

$$y = \ln \ln \left(\frac{1}{1-CDF}\right) \tag{B-4}$$

$$x = \ln (d_p - d_{po}) \tag{B-5}$$

which means that:

$$A = -b \ln (\Theta - d_{po}) \tag{B-6}$$

$$B = b \tag{B-7}$$

or,

$$\Theta = d_{po} + \exp \left(-\frac{A}{B}\right) \tag{B-8}$$

$$b = B \tag{B-9}$$

Least Squares Curve Fit

The minimum particle diameter, d_{po}, is that which results in the highest linear correlation coefficient based on the above linear transformation, when a least squares linear regression is performed on the size distribution data. Note that,

$0 \leq d_{po} <$ smallest diameter found in the distribution

Density Function

The Weibull density function is the derivative of the CDF:

$$f(d_p) = \frac{b}{\Theta - d_{po}} \left(\frac{d_p - d_{po}}{\Theta - d_{po}}\right)^{b-1} \exp \left[-\left(\frac{d_p - d_{po}}{\Theta - d_{po}}\right)^b\right] \tag{B-10}$$

Penetration

The penetration is the ratio of the cumulative mass loading distribution derivatives,

$$Pt\ (d_p) = \frac{C_{T,out}\ f_{out}\ (d_p)}{C_{T,in}\ f_{in}\ (d_p)} \qquad \text{(B-11)}$$

where, C_T = total mass concentration or loading

"out" - refers to outlet particle size distribution

"in" - refers to inlet particle size distribution

and, $f(d_p)$ - is defined by equation (B-10)

Minimum Particle Diameter, Physical Interpretation

"d_{po}" is the smallest diameter of the total distribution. A value other than zero means that the data indicate that there is a minimum particle size. This is physically reasonable because of the particle formation mechanisms and possible agglomeration and/or particle growth.

Characteristic Diameter, Physical Interpretation

"Θ" is analogous to the geometric mean particle diameter of the log-probability distribution and is therefore an indication of the "average" size of the particles in the distribution. The median particle diameter is directly related to "Θ" by equation (B-2).

Weibull Slope, Physical Interpretation

"b" is analogous to the geometric standard deviation of the log-probability distribution. It indicates the "spread" of the size distribution. The larger the Weibull slope, b, the more uniform (monodisperse) the particle sizes.

APPENDIX C

Venturi Performance Model

VENTURI SCRUBBER PERFORMANCE MODEL

Yung, et al., 1977* have performed a literature review and evaluation of all available venturi scrubber performance models. Their conclusions and recommended performance model are presented below.

(1) Even though each investigator presented a different equation for the prediction of particle collection in a venturi scrubber, most of these equations can be reduced to the same basic model, i.e.,

$$-\ln Pt\ (d_p) = \int_o^z \frac{3\ u_r\ Q_w\ \eta}{2\ u_G\ (u_G - u_r)\ d_d}\ dz \qquad \text{(C-1)}$$

where $Pt(d_p)$ = penetration for particles with diameter d_p, fraction

u_r = relative velocity between dust and drop, cm/sec

u_G = gas velocity, cm/sec

d_d = drop diameter, cm

η = single drop collection efficiency, fraction

Q_w = liquid volumetric flow rate, cm^3/sec

z = length, cm

(2) A generalized method for applying equation C-1 to predict particle collection in a venturi was developed.

(3) Particle collection predicted by equation C-1 agrees satisfactorily with performance data.

(4) Most of the particle collection occurs in the venturi throat. The solution to equation C-1 for the venturi throat, using the inertial collection efficiency correlation, and assuming a zero initial drop velocity, is

*Yung, S., S. Calvert, and H.F. Barbarika, "Venturi Scrubber Performance Model, EPA 600/2-77-172, A.P.T., Inc., San Diego, California, 1977.

$$\frac{\ln Pt(d_p)}{B} = \frac{1}{K_{po}\left(1-u_d^*\right)+0.7}\left[4\,K_{po}\left(1-u_d^*\right)^{1.5} + 4.2\left(1-u_d^*\right)^{0.5}\right.$$

$$\left. - 5.02\,K_{po}^{0.5}\left(1-u_d^* + \frac{0.7}{K_{po}}\right)\tan^{-1}\left(\frac{\left(1-u_d^*\right)K_{po}}{0.7}\right)^{0.5}\right]$$

$$- \frac{1}{K_{po} + 0.7}\left[4\,K_{po} + 4.2 - 5.02\,K_{po}^{0.5}\left(1 + \frac{0.7}{K_{po}}\right)\tan^{-1}\left(\frac{K_{po}}{0.7}\right)^{0.5}\right.$$

(C-2)

where $u_d^* = 2\left\{1 - \left(\frac{L+8}{8}\right)^2 + \left(\frac{L+8}{8}\right)\left[\left(\frac{L+8}{8}\right)^2 - 1\right]^{0.5}\right\}$

$Pt(d_p)$ = penetration for particles with diameter d_p, fraction

$B = \left(\frac{Q_L}{Q_G}\right)\left(\frac{\rho_L}{\rho_G}\right)\frac{1}{C_{Do}}$

Q_L = volumetric liquid flow rate, cm^3/sec

ρ_L = liquid density, g/cm^3

ρ_G = gas density, g/cm^3

C_{Do} = drag coefficient obtained from the "standard curve

u_d^* = dimensionless drop velocity

$= \frac{u_d}{u_{Gt}}$

u_d = drop velocity, cm/sec

u_{Gt} = gas velocity in the throat, cm/sec

K_{po} = inertial parameter based on throat velocity

$= \frac{C' d_p^2 \rho_p u_{Gt}}{9 \mu_G d_d}$

C' = Cunningham slip factor
d_p = particle diameter, μm
ρ_p = particle density, g/cm³
μ_G = gas viscosity, poise
d_d = drop diameter, cm
L = dimensionless throat length

$$L = \frac{3\ \ell_t\ C_{Do}\ \rho_G}{2\ d_d\ \rho_L}$$

Equation C-2 slightly under estimates the particle collection occurring in a venturi scrubber. For most industrial venturi scrubbers, particle collection can be predicted closely by neglecting the first term in the right hand side of equation C-2.

(5) Pressure drop predictions by the modified Calvert's equation and by Boll's equation agree with experimental data. The modified Calvert's equation has the following form,

$$\Delta P = 1.03 \times 10^{-3}\ F_1\ u_{Gt}^2 \left(\frac{Q_L}{Q_G}\right) \qquad \text{(C-3)}$$

where ΔP = pressure, cm W.C.
u_{Gt} = gas velocity in the throat, cm/sec
Q_L = liquid flow rate, cm³/sec
Q_G = gas-flow rate, cm³/sec
F_1 = correction factor, dimensionless

$$F_1 = \frac{u_{de}}{u_{Gt}} = 2\left[1 - X^2 + (X^4 - X^2)^{0.5}\right]$$

$$X = \frac{3\ \ell_t C_{Do}\ \rho_G}{16\ d_d\ \rho_L} + 1$$

u_{de} = drop velocity at the exit of the throat, cm/sec

ℓ_t = throat length or distance between liquid injection point and the exit of throat, cm

d_d = drop diameter, cm

ρ_G = gas density, g/cm^3

ρ_L = liquid density, g/cm^3

C_{Do} = drag coefficient at the liquid injection point.

(6) The use of a drag coefficient from the "Standard curve" gives a better fit between model and experimental data than does Ingebo's correlation.

(7) The drop diameter can be assumed to be the Sauter mean diameter calculated from the Nukiyama-Tanasawa relation.

TECHNICAL REPORT DATA
(Please read Instructions on the reverse before completing)

1. REPORT NO. EPA-600/2-77-209a	2.
3. RECIPIENT'S ACCESSION NO.	
4. TITLE AND SUBTITLE Gas-atomized Spray Scrubber Evaluation	5. REPORT DATE October 1977
	6. PERFORMING ORGANIZATION CODE
7. AUTHOR(S) Seymour Calvert, Harry F. Barbarika, and Gary M. Monahan	8. PERFORMING ORGANIZATION REPORT NO.
9. PERFORMING ORGANIZATION NAME AND ADDRESS Air Pollution Technology, Inc. 4901 Morena Boulevard (Suite 402) San Diego, California 92117	10. PROGRAM ELEMENT NO. 1AB012; ROAP 21ADM-029
	11. CONTRACT/GRANT NO. 68-02-1869
12. SPONSORING AGENCY NAME AND ADDRESS EPA, Office of Research and Development Industrial Environmental Research Laboratory Research Triangle Park, NC 27711	13. TYPE OF REPORT AND PERIOD COVERED Task Final; 2-8/77
	14. SPONSORING AGENCY CODE EPA/600/13

15. SUPPLEMENTARY NOTES IERL-RTP project officer for this report is Dale L. Harmon, Mail Drop 61, 919/541-2925. EPA-600/2-76-282 is an earlier report in this series.

16. ABSTRACT The report gives results of fine particle collection efficiency measurements of a gas-atomized spray scrubber, cleaning effluent gas from a No. 7 gray iron cupola. Tests were made at several levels of pressure drop and liquid/gas ratio. Particle size measurements on inlet and outlet gas streams were made with cascade impactors and an A. P. T. screen-type diffusion battery. The particle mass collection efficiency at a pressure drop of about 100 cm W.C. was 91% for particles with a mass median diameter of about 0.4 micrometers A. Scrubber inlet gas flow rate varied, because the cupola was operated with an open top, from 4.0 to 12.6 A cu m/s (8,500 to 27,000 acfm). Air leakage into the scrubber system caused serious operating problems until most of the leaks were sealed. The penetrations for 1 micrometer A diameter particles were about as predicted by the mathematical model; however, smaller particle penetrations were lower, and larger particle penetrations were higher, than predicted. The latter two effects are believed due to water condensation effects and entrainment, respectively.

17. KEY WORDS AND DOCUMENT ANALYSIS

a. DESCRIPTORS	b. IDENTIFIERS/OPEN ENDED TERMS	c. COSATI Field/Group
Air Pollution Iron and Steel Industry Dust Measurements Gray Iron Furnace Cupolas Scrubbers Atomizing Spraying	Air Pollution Control Stationary Sources Particulate Collection Efficiency Gas-atomized Spray Scrubber	13B 13H 11F 11G 14B 07A

18. DISTRIBUTION STATEMENT Unlimited	19. SECURITY CLASS *(This Report)* Unclassified	21. NO. OF PAGES 77
	20. SECURITY CLASS *(This page)* Unclassified	22. PRICE

EPA Form 2220-1 (9-73)